(39). The results are consistent with the observation that *H. pylori* rarely colonizes the layer where gland mucous cell-derived mucins are present (2). These combined results suggest that the expression of sialyl Lewis X may facilitate *H. pylori* infection and resultant inflammation, whereas α1,4-GlcNAc-capped O-glycans in the gland mucous cells inhibits this process.

The present study also demonstrated that HEV-like vessels disappear once *H. pylori* is eradicated by antibiotic treatment. The results indicate that the formation of HEV-like vessels and thus recruitment of lymphocytes to chronic inflammatory sites in the gastric mucosa can be reversed once *H. pylori* infection is abolished. It is tempting to speculate that lipopolysaccharides and/or other components from the organism, acting through Toll-like receptor-dependent pathways in the gastric epithelium, exerts the elaboration of cytokines, i.e., lymphotoxin α. This effect might in turn modulate gene expression in postcapillary venules in ways that cause their biochemical, functional, and morphological transformation by up-regulating chemokines, such as CCL19 and CCL21, that act on CCR7 receptors.

Several enzymes play major roles in the biosynthesis of PNAd at the secondary lymphoid organs, including LSST (also called GlcNAc6ST-2 or HEC-GlcNAc6ST) (30, 40), Core2GlcNAcT-I (21, 31), and Core1-β3GlcNAcT (21, 32). Mice that are mutant in any of these enzymes exhibit reduced lymphocyte homing activity compared with wild-type mice (31, 32, 40). Future studies that determine whether inhibition of L-selectin ligand synthesis can inhibit the chronic inflammation induced by *H. pylori* infection and, hence, the formation of gastric carcinoma would be of great interest. Mice with targeted mutations in various glycosyltransferases and sulfotransferases responsible for L-selectin ligand synthesis will likely provide critical tools for those studies.

We thank Yasuyo Shimojo and Akiko Ishida for preparation of tissue sections, Dr. John Lowe (University of Michigan Medical School, Ann Arbor) for providing pcDNA1-P-selectin-IgM, Dr. Elise Lamar for critical reading of the manuscript, Yoav Altman for assisting in FACS analysis, and Aleli Morse for organizing the manuscript. This work was supported by the National Institutes of Health Grant R37 CA33000 (to M.F.) and by Ministry of Education, Culture, Sports, Science, and Technology of Japan Priority Area 14082201 and the Ministry of Health, Labor, and Welfare of Japan (Third Term Comprehensive Control Research for Cancer) (to J.N.).

1. Marshall, B. J. & Warren, J. R. (1984) *Lancet* **i**, 1311–1315.
2. Hidaka, E., Ota, H., Hidaka, H., Hayama, M., Matsuzawa, K., Akamatsu, T., Nakayama, J. & Katsuyama, T. (2001) *Gut* **49**, 474–480.
3. Sipponen, P. & Hyvarinen, H. (1993) *Scand. J. Gastroentrol.*, Suppl., **196**, 3–6.
4. Peek, R. M., Jr. & Blaser, M. J. (2002) *Nat. Rev. Cancer* **2**, 28–37.
5. Yuasa, Y. (2003) *Nat. Rev. Cancer* **3**, 592–600.
6. Freund, J. N., Domon-Dell, C., Kedinger, M. & Duluc, I. (1998) *Biochem. Cell. Biol.* **76**, 957–969.
7. Hinoi, T., Lucas, P. C., Kuick, R., Hanash, S., Cho, K. R. & Fearon, E. R. (2002) *Gastroenterology* **123**, 1565–1577.
8. Bayerdorffer, E., Neubauer, A., Rudolph, B., Thiede, C., Lehn, N., Eidt, S. & Stolte, M. (1995) *Lancet* **345**, 1591–1594.
9. Nomura, A., Stemmermann, G. N., Chyou, P. H., Kato, I., Perez-Perez, G. I. & Blaser, M. J. (1991) *N. Engl. J. Med.* **325**, 1132–1136.
10. Parsonnet, J., Freidman, G. D., Vandersteen, D. P., Chang, Y., Vogelman, J. H., Orentreich, N. & Sibley, R. K. (1991) *N. Engl. J. Med.* **325**, 1127–1131.
11. Higashi, H., Tsutsumi, R., Muto, S., Sugiyama, T., Azuma, T., Asaka, M. & Hatakeyama, M. (2002) *Science* **295**, 683–686.
12. Rosen, S. D. (2004) *Annu. Rev. Immunol.* **22**, 129–156.
13. von Andrian, U. H. & Mackay, C. R. (2000) *N. Engl. J. Med.* **343**, 1020–1034.
14. Duijvestijn, A. M., Kerkhove, M., Bargatze, R. F. & Butcher, E. C. (1987) *J. Immunol.* **138**, 713–719.
15. Kabel, P. J., Voorbij, H. A., de Haan-Meulman, M., Pals, S. T. & Drexhage, H. A. (1989) *J. Clin. Endocrinol. Metab.* **68**, 744–751.
16. van Dinther-Janssen, A. C., Pals, S. T., Scheper, R., Breedveld, F. & Meijer, C. J. (1990) *J. Rheumatol.* **17**, 11–17.
17. Salmi, M., Granfors, K., MacDermott, R. & Jalkanen, S. (1994) *Gastroenterology* **106**, 596–605.
18. Streeter, P. R., Rouse, B. T. & Butcher, E. C. (1988) *J. Cell. Biol.* **107**, 1853–1862.
19. Mazzucchelli, L., Blaser, A., Kappeler, A., Schärli, P., Laissue, J. A., Baggiolini, M. & Uguccioni, M. (1999) *J. Clin. Invest.* **104**, R29–R54.
20. Dogan, A., Du, M., Koulis, A., Briskin, M. J. & Isaacson, P. G. (1997) *Am. J. Pathol.* **151**, 1361–1369.
21. Yeh, J. C., Hiraoka, N., Petryniak, B., Nakayama J., Ellies, L. G., Rabuka, D., Hindsgaul, O., Marth, J. D., Lowe, J. B. & Fukuda, M. (2001) *Cell* **105**, 957–969.
22. Hemmerich, S., Leffler, H. & Rosen, S. D. (1995) *J. Biol. Chem.* **270**, 12035–12047.
23. Duijvestijn, A. M., Horst, E., Pals, S. T., Rouse, B. N., Steere, A. C., Picker, L. J., Meijer, C. J. & Butcher, E. C. (1988) *Am. J. Pathol.* **130**, 147–155.
24. Kumamoto, K., Mitsuoka, C., Izawa, M., Kimura, N., Otsubo, N., Ishida, H., Kiso, M., Yamada, T., Hirohashi, S. & Kannagi, R. (1998) *Biochem. Biophys. Res. Commun.* **247**, 514–517.
25. Dixon, M. F., Genta, R. M., Yardley, J. H. & Correa, P. (1996) *Am. J. Surg. Pathol.* **20**, 1161–1181.
26. Taha, A. S., Nakshabendi, I., Lee, F. D., Sturrock, R. D. & Russel, R. I. (1992) *J. Clin. Pathol.* **45**, 135–139.
27. Dixon, M. F., O'Connor, H. J., Axon, A. T., King, R. F. & Johnston, D. (1986) *J. Clin. Pathol.* **39**, 524–530.
28. Renkonen, J., Tynninen, O., Hayry, P., Paavonen, T. & Renkonen, R. (2002) *Am. J. Pathol.* **161**, 543–550.
29. Maly, P., Thall, A., Petryniak, B., Rogers, C. E., Smith, P. L., Marks, R. M., Kelly, R. J., Gersten, K. M., Cheng, G., Saunders, T. L., *et al.* (1996) *Cell* **86**, 643–653.
30. Hiraoka, N., Petryniak, B., Nakayama, J., Tsuboi, S., Suzuki, M., Yeh, J. C., Izawa, D., Tanaka, T., Miyasaka, M., Lowe, J. B. & Fukuda, M. (1999) *Immunity* **11**, 79–89.
31. Hiraoka, N., Kawashima, H., Petryniak, B., Nakayama, J., Mitoma, J., Marth, J. D., Lowe, J. B. & Fukuda, M. (2004) *J. Biol. Chem.* **279**, 3058–3067.
32. Mitoma, J., Petryniak, B., Hiraoka, N., Yeh, J. C., Lowe, J. B. & Fukuda, M. (2003) *J. Biol. Chem.* **278**, 9953–9961.
33. Mitsuoka, C., Kawakami-Kimura, N., Kasugai-Sawada, M., Hiraiwa, N., Toda, K., Ishida, H., Kiso, M., Hasegawa, A. & Kannagi, R. (1997) *Biochem. Biophys. Res. Commun.* **230**, 546–551.
34. Toppila, S., Paavonen, T., Nieminen, M. S., Häyry, P. & Renkonen, R. (1999) *Am. J. Pathol.* **155**, 1303–1310.
35. Fukuda, M., Carlsson, S. R., Klock, J. C. & Dell, A. (1986) *J. Biol. Chem.* **261**, 12796–12806.
36. Wilkins, P. P., McEver, R. P. & Cummings, R. D. (1996) *J. Biol. Chem.* **271**, 18732–18742.
37. Mahdavi, J., Sonden, B., Hurtig, M., Olfat, F. O., Forsberg, L., Roche, N., Angstrom, J., Larsson, T., Teneberg, S., Karlsson, K. A., *et al.* (2002) *Science* **297**, 573–578.
38. Guruge, J. L., Falk, P. G., Lorenz, R. G., Dans, M., Wirth, H. P., Blaser, M. J., Berg, D. E. & Gordon, J. I. (1998) *Proc. Natl. Acad. Sci. USA* **95**, 3925–3930.
39. Kawakubo, M., Ito, Y., Okimura, Y., Kobayashi, M., Sakura, K., Kasama, S., Fukuda, M. N., Fukuda, M., Katsuyama, T. & Nakayama, J. (2004) *Science* **305**, 1003–1006.
40. Hemmerich, S., Bistrup, A., Singer, M. S., van Zante, A., Lee, J. K., Tsay, D., Peters, M., Carminati, J. L., Brennan, T. J., Carver-Moore, K., *et al.* (2001) *Immunity* **15**, 237–247.

nature immunology

N-acetylglucosamine-6-*O*-sulfotransferases 1 and 2 cooperatively control lymphocyte homing through L-selectin ligand biosynthesis in high endothelial venules

Hiroto Kawashima[1], Bronislawa Petryniak[2], Nobuyoshi Hiraoka[1], Junya Mitoma[1], Valerie Huckaby[1], Jun Nakayama[3], Kenji Uchimura[4], Kenji Kadomatsu[4], Takashi Muramatsu[4], John B Lowe[2] & Minoru Fukuda[1]

Lymphocyte homing is mediated by specific interactions between L-selectin on lymphocytes and sulfated carbohydrates restricted to high endothelial venules in lymph nodes. Here we generated mice deficient in both *N*-acetylglucosamine-6-*O*-sulfotransferase 1 (GlcNAc6ST-1) and GlcNAc6ST-2 and found that mutant mice had approximately 75% less homing of lymphocytes to the peripheral lymph nodes than did wild-type mice. Consequently, these mice had lower contact hypersensitivity responses than those of wild-type mice. Carbohydrate structural analysis showed that 6-sulfo sialyl Lewis X, a dominant ligand for L-selectin, was almost completely absent from the high endothelial venules of these mutant mice, whereas the amount of unsulfated sialyl Lewis X was much greater. These results demonstrate the essential function of GlcNAc6ST-1 and GlcNAc6ST-2 in L-selectin ligand biosynthesis in high endothelial venules and their importance in immune surveillance.

Lymphocytes encounter antigens derived from foreign pathogens and initiate immune responses in secondary lymphoid organs such as lymph nodes and Peyer's patches. Therefore, homing of lymphocyte to secondary lymphoid organs is an essential process for immune surveillance. Lymphocyte homing is critically dependent on a specific interaction between the lymphocyte-homing receptor L-selectin and its ligands, whose expression is restricted to high endothelial venules (HEVs) in the lymph nodes[1]. This adhesive interaction mediates lymphocyte tethering and rolling on the surface of HEVs, which is a prerequisite for the subsequent lymphocyte chemokine-dependent activation, integrin-mediated firm attachment to the endothelium and transmigration across blood vessels[2–5].

L-selectin is a carbohydrate-binding protein that binds to its ligands on HEVs in a calcium-dependent way. HEV-restricted ligands for L-selectin include GlyCAM-1, CD34, podocalyxin-like protein, Sgp200, endoglycan and MAdCAM-1, all of which have mucin-like domains that act as scaffolding for *O*-glycans[6]. The ability of these ligands to function entirely depends on their 'decoration' with specific carbohydrate structures, including 6-sulfo sialyl Lewis X (sialyl-α(2-3)-galactopyranosyl-β(1-4)-[fucopyranosyl-α(1-3)(sulfo-6)]-*N*-acetylglucosamine) which contains fucose, sialic acid and sulfate[6].

The pivotal function of fucosylation of L-selectin ligands for their interaction with L-selectin has been established by genetic studies of mice. Mice deficient in fucosyltransferase VII (FucT-VII) have a reduction of nearly 80% in homing of lymphocytes to the peripheral lymph nodes, indicating that FucT-VII is the principal enzyme involved in fucosylation of L-selectin ligands on HEVs[7]. Studies using mice doubly deficient in both FucT-VII and FucT-IV have demonstrated an additional function for FucT-IV in HEV ligand fucosylation[8]. The essential involvement of sialylation of L-selectin ligands has also been demonstrated by experiments showing sialidase treatment of lymph node sections completely abrogates L-selectin-dependent binding of lymphocytes to HEVs in peripheral lymph nodes[9].

Sulfation of L-selectin ligands is important in the interaction with L-selectin *in vitro*. An initial demonstration of such a requirement showed that treatment of lymph node organ culture with chlorate, an inhibitor of sulfation, abrogates interaction between recombinant L-selectin and its glycoprotein ligands[10,11]. Subsequently, the use of a specific antibody identified the main capping group of L-selectin ligands on HEVs in human lymph nodes as 6-sulfo sialyl Lewis X[12]. The HEV-restricted sulfotransferase *N*-acetylglucosamine-6-*O*-sulfotransferase-2 (GlcNAc6ST-2, also called HEC-GlcNAc6ST or L-selectin ligand sulfotransferase) has been cloned and participates in the biosynthesis of 6-sulfo sialyl Lewis X and can reconstitute the L-selectin ligand *in vitro*[13,14]. Furthermore, the 6-sulfo sialyl Lewis X structure is present in either the core 2 or extended core 1 branch or in both branches of L-selectin ligand *O*-glycans[15]. Moreover, the MECA-79 antibody[16], which is widely used to detect HEVs in lymph nodes or HEV-like vessels at the sites of chronic inflammation, recognizes *O*-glycans containing 6-sulfo *N*-acetylglucosamine in the extended

[1]Glycobiology Program, Cancer Research Center, The Burnham Institute, La Jolla 92037, California, USA. [2]Howard Hughes Medical Institute, Life Sciences Institute, University of Michigan Medical School, Ann Arbor, Michigan 48109, USA. [3]Department of Pathology, Shinshu University School of Medicine, Matsumoto 390-8621, Japan. [4]Department of Biochemistry, Nagoya University School of Medicine, Nagoya 466-8550, Japan. Correspondence should be addressed to M.F. (minoru@burnham.org).

Received 19 June; accepted 25 August; published online 9 October 2005; doi:10.1038/ni1259

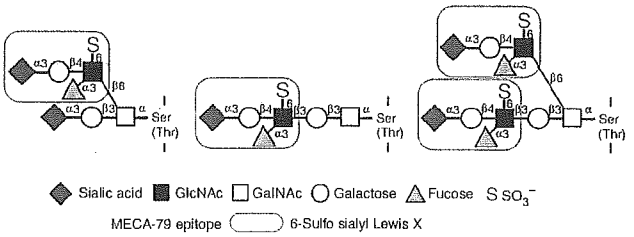

Figure 1 L-selectin ligand oligosaccharides. Core 2–branched *O*-glycan (left), extended core 1 structure (middle) and biantennary *O*-glycan containing both a core 2 branch and an extended core 1 structure (right) modified with 6-sulfo sialyl Lewis X (gray outlined areas) function as L-selectin ligand oligosaccharides in HEVs. The extended core 1 structures modified with GlcNAc-6-*O*-sulfate (yellow shaded areas) are recognized by MECA-79 (ref. 15). Each Greek character and number represents a carbohydrate linkage.

core 1 structure[15]. Although those studies have indicated a sulfation requirement of HEV-borne carbohydrates as L-selectin ligands *in vitro*, that requirement has not been demonstrated *in vivo*.

For assessment of the function of the sulfation of L-selectin ligands *in vivo*, mutant mice deficient in the HEV-restricted sulfotransferase GlcNAc6ST-2 have been generated[17,18]. In these mice, the binding of MECA-79 to lymph node HEVs is substantially diminished, except for binding in the lining of HEVs on the surface away from the lumen, suggesting that the GlcNAc-6-*O*-sulfation in the extended core 1 branch is mediated mainly by GlcNAc6ST-2. Oligosaccharide structural analysis has indicated that GlcNAc-6-*O*-sulfation in the extended core 1 structure on GlyCAM-1 is substantially less in GlcNAc6ST-2–deficient mice than in wild-type mice[17]; however, the GlcNAc-6-*O*-sulfation in the core 2–branched *O*-glycan persists in GlcNAc6ST-2–deficient mice. Consistent with that observation, there is only partial disruption of lymphocyte homing (approximately 50%) in GlcNAc6ST-2–deficient mice[17,18].

Four mouse GlcNAc-6-*O*-sulfotransferases have been identified[19,20]. GlcNAc6ST-1 is widely expressed in various tissues, including lymph node HEVs[21], and functions in L-selectin ligand biosynthesis *in vitro*[22] and *in vivo*[23]. GlcNAc6ST-1–deficient mice have a reduction of an approximately 20% in homing of lymphocytes to peripheral lymph nodes[23], suggesting that GlcNAc6ST-1 and GlcNAc6ST-2 might have overlapping or complementary functions. To determine the sulfation requirement of L-selectin ligands *in vivo* in further detail, we generated mice deficient in both GlcNAc6ST-1 and GlcNAc6ST-2 and show here that these sulfotransferases cooperatively have a chief function in L-selectin ligand biosynthesis in HEVs. Systematic carbohydrate analysis of an HEV-specific glycoprotein showed that essentially no 6-sulfo sialyl Lewis X structure was synthesized in the HEVs of mice deficient in both GlcNAc6ST-1 and GlcNAc6ST-2 ('double-knockout' mice), but that the amount of the unsulfated sialyl Lewis X structure was up to sevenfold greater than that in wild-type mice. Moreover, contact hypersensitivity responses were substantially diminished in the double-knockout mice because of a reduction in lymphocyte trafficking to the draining lymph nodes. Our study provides a link between the structural alterations of carbohydrates in HEVs and lymphocyte recruitment in health and disease.

RESULTS

Expression of L-selectin ligands in HEVs

To determine the expression of L-selectin-reactive carbohydrates in HEVs of mutant mice, we did immunofluorescence studies using MECA-79 and an L-selectin–immunoglobulin M (L-sel–IgM) chimeric protein. MECA-79 recognizes extended core 1 structures modified with GlcNAc-6-*O*-sulfate, whereas L-selectin interacts with various *O*-glycans modified with 6-sulfo sialyl Lewis X present in HEVs[15] (**Fig. 1**). Binding of MECA-79 to HEVs in peripheral lymph nodes and mesenteric lymph nodes was completely abolished in double-knockout mice (**Fig. 2a**). Only expression of enhanced green fluorescent protein (EGFP), which replaced the catalytic domain and stem region of GlcNAc6ST-2 in the targeting vector[17], was detectable in HEVs. In Peyer's patches of mice deficient in GlcNAc6ST-1 alone, MECA-79 staining was undetectable, consistent with published results[23]. In contrast, the binding of L-sel–IgM to HEVs of peripheral lymph nodes and mesenteric lymph nodes was not completely abolished in the double-knockout mice, although it was substantially reduced relative to that of wild-type mice or mice deficient in either GlcNAc6ST-1 or GlcNAc6ST-2 (**Fig. 2b**). These results indicated that GlcNAc-6-*O*-sulfation in the extended core 1 branch of *O*-glycans was

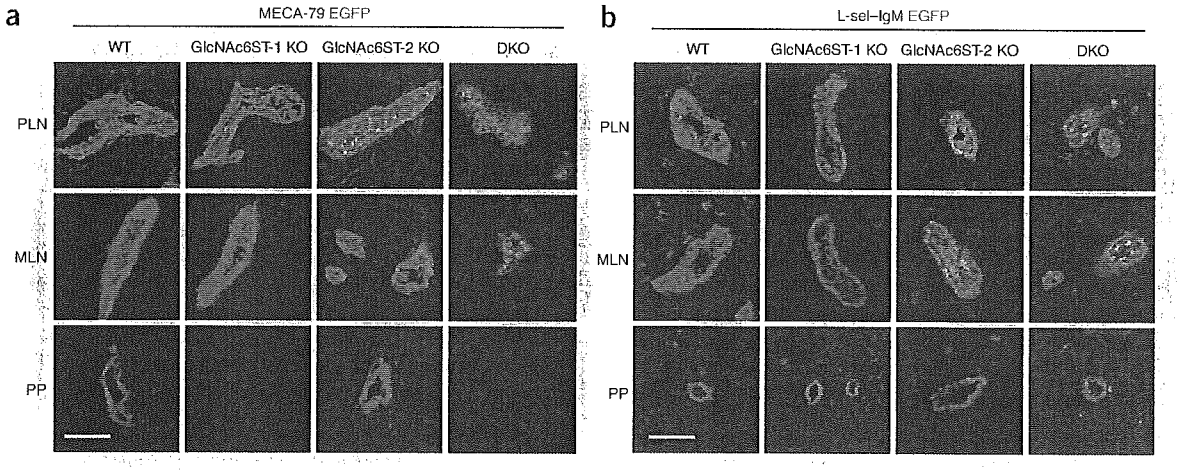

Figure 2 Expression of MECA-79 antigen, L-selectin ligands and the GlcNAc6ST-2–EGFP chimeric protein. Frozen sections (7 μm in thickness) of peripheral lymph nodes (PLN), mesenteric lymph nodes (MLN) and Peyer's patches (PP) from wild-type (WT), GlcNAc6ST-1–deficient (GlcNAc6ST-1 KO), GlcNAc6ST-2–deficient (GlcNAc6ST-2 KO) and double-knockout (DKO) mice were stained with MECA-79 (red in **a**) or L-sel–IgM (red in **b**). Green fluorescence is from the GlcNAc6ST-2–EGFP chimeric protein[17]. Scale bars, 50 μm. Data are representative of ten independent experiments.

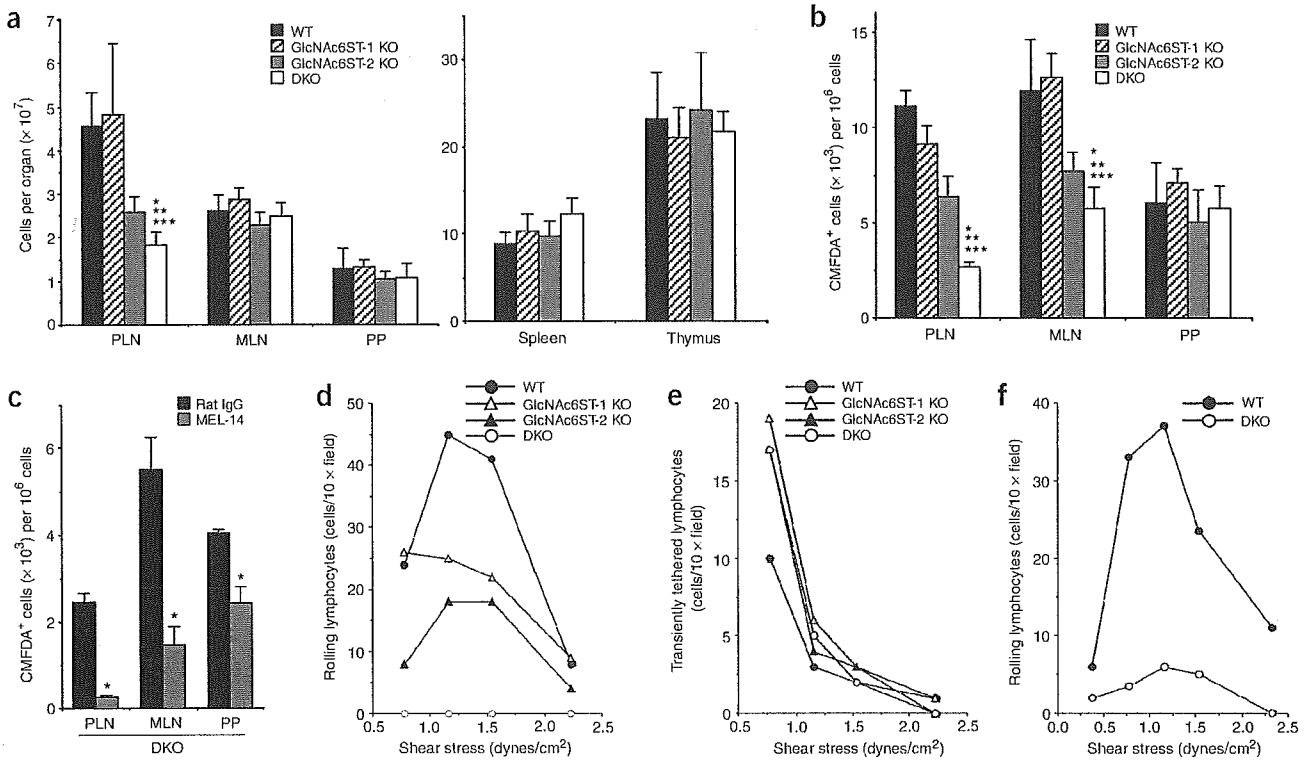

Figure 3 Lymphocyte trafficking to secondary lymphoid organs. **(a)** Lymphocytes recovered from lymphoid organs of 7-week-old wild-type and null mice ($n = 5$–7 mice). *, $P < 0.01$, versus wild-type mice; **, $P < 0.01$, versus GlcNAc6ST-1-deficient mice; ***, $P < 0.02$, versus GlcNAc6ST-2-deficient mice. **(b,c)** Flow cytometry of lymphocytes in lymphoid organs. CMFDA-labeled lymphocytes (2.5×10^7 cells) were injected into tail veins of wild-type and null mice **(b)** or CMFDA-labeled lymphocytes (2.5×10^7 cells) incubated with 30 μg of MEL-14 (rat IgG2a) or rat IgG were injected into tail veins of double-knockout mice **(c)**. Then, 1 h later, fluorescent lymphocytes in lymphocyte suspensions from lymphoid organs were quantified. At least four recipient mice were tested in each experiment. **(b)** For PLN, *, $P < 0.01$, versus wild-type mice; **, $P < 0.01$, versus GlcNAc6ST-1-deficient mice; ***, $P < 0.01$, versus GlcNAc6ST-2-deficient mice. For MLN, *, $P < 0.01$, versus wild-type mice; **, $P < 0.01$, versus GlcNAc6ST-1-deficient mice; ***, $P < 0.1$, versus GlcNAc6ST-2-deficient mice. **(c)** *, $P < 0.01$, versus rat IgG-injected mice. **(d–f)** Lymphocyte rolling assay on GlyCAM-1 from various mouse lines captured by antibody to GlyCAM-1 at concentrations of 20 μg/ml **(d,e)** and 50 μg/ml **(f)**. Data are representative of three **(b,c)** or two **(d–f)** independent experiments.

abrogated in double-knockout mice but that L-selectin-reactive carbohydrates were still expressed in low abundance.

Lymphocyte trafficking to lymph nodes

We next determined whether lymphocyte homing was affected in double-knockout mice. The number of lymphocytes in peripheral lymph nodes was reduced by 60% in double-knockout mice compared with that in wild-type mice (**Fig. 3a**). In a short-term homing assay, mice deficient in either GlcNAc6ST-1 or GlcNAc6ST-2 had a reduction of approximately 20% or 50%, respectively, in homing of lymphocytes to peripheral lymph nodes, whereas double-knockout mice had a reduction of approximately 75% (**Fig. 3b**). The residual homing of lymphocytes to peripheral lymph nodes in double-knockout mice was apparently mediated by L-selectin, as it was reduced to background by MEL-14, an antibody blocking L-selectin function (**Fig. 3c**). Lymphocyte homing to mesenteric lymph nodes and Peyer's patches was only partially blocked by MEL-14, possibly because interactions between $\alpha_4\beta_7$ integrin and MAdCAM-1 are also involved in homing of lymphocytes to these secondary lymphoid organs[24].

The additive reduction in lymphocyte homing in the double-knockout mice was consistent with results of an *in vitro* rolling assay, in which we applied normal lymphocytes to flow chambers coated with GlyCAM-1, an HEV-specific secreted glycoprotein, from the sera of wild-type or mutant mice (**Fig. 3d–f**). We noted no lymphocyte rolling when we used lymphocytes from L-selectin-deficient mice in this assay (data not shown), indicating that the rolling was mediated exclusively by L-selectin. GlyCAM-1 derived from mutant mice deficient in either GlcNAc6ST-1 or GlcNAc6ST-2 supported less lymphocyte rolling than that from wild-type mice (**Fig. 3d**). GlyCAM-1 derived from double-knockout mice did not support lymphocyte rolling when a low density of GlyCAM-1 was used. However, there were many transiently tethered lymphocytes in the same conditions (**Fig. 3e**), suggesting that the initial tethering of lymphocytes is less affected than the rolling velocity in double-knockout mice. GlyCAM-1 derived from double-knockout mice weakly supported rolling when we used a high density of GlyCAM-1 (**Fig. 3d** versus **f**), further supporting the idea that these mice have only weak L-selectin ligand activity.

Contact hypersensitivity response

To determine the relevance of GlcNAc6ST-1 and GlcNAc6ST-2 in immune responses in pathophysiological settings, we assessed contact hypersensitivity responses in mutant mice. Double-knockout mice showed significant reductions in ear swelling and leukocyte infiltration after sensitization and challenge with the hapten DNFB (2,4-dinitrofluorobenzene; **Fig. 4a,b**). HEV-like vessels reactive with MECA-79 or

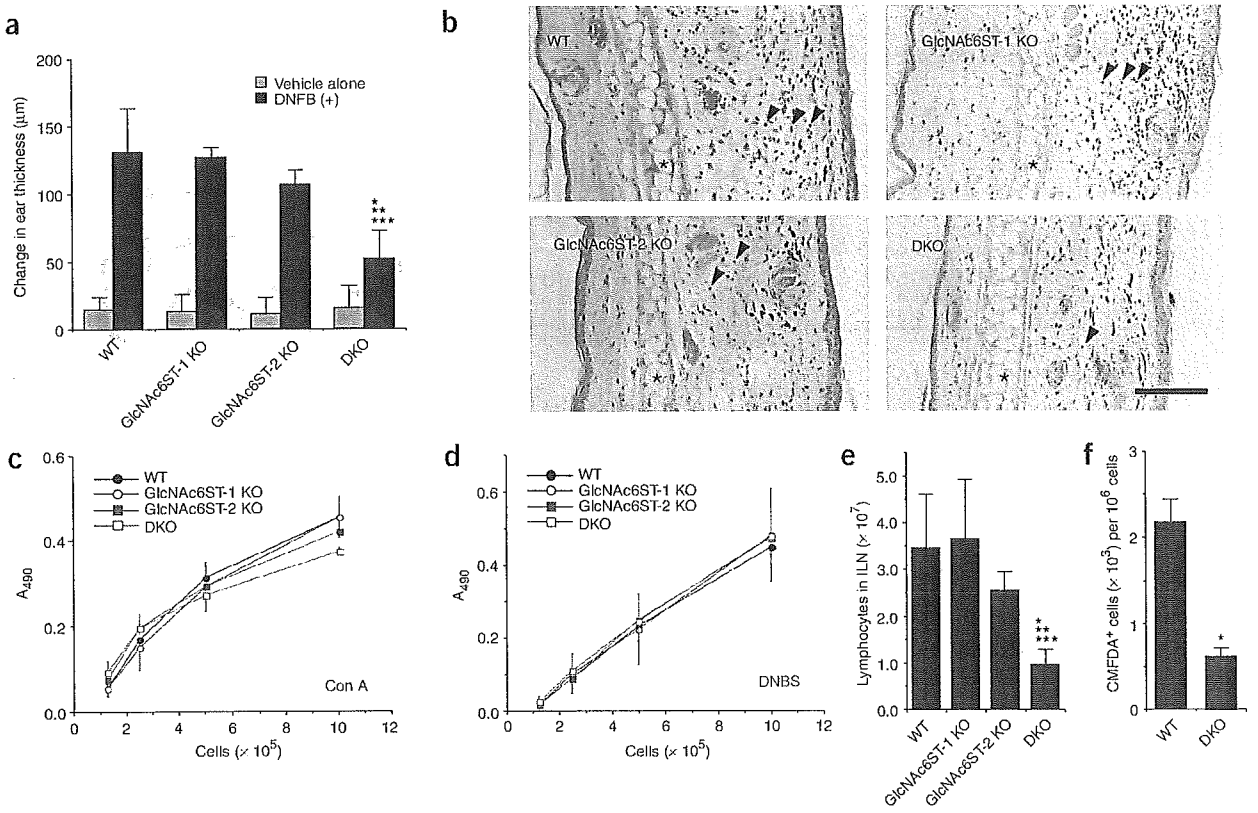

Figure 4 Reduced contact hypersensitivity in the double-knockout mice. **(a)** Ear swelling 24 h after challenge with DNFB or vehicle alone in wild-type and null mice (horizontal axis; $n = 5$). *, $P < 0.01$, versus wild-type mice; **, $P < 0.01$, versus GlcNAc6ST-1-deficient mice; ***, $P < 0.01$, versus GlcNAc6ST-2-deficient mice. **(b)** Hematoxylin-and-eosin staining of ear sections 24 h after DNFB challenge. *, ear cartilage; arrowheads, recruited leukocytes. Scale bar, 100 μm. **(c,d)** Cell proliferation assay of lymphocytes from inguinal lymph nodes sensitized with DNFB and cultured in the presence of concanavalin A (Con A; 2 μg/ml) or DNBS (200 μg/ml; $n = 3$ mice). A_{490}, absorbance at 490 nm. **(e)** Lymphocytes recovered from the inguinal lymph nodes (ILN) of DNFB-sensitized mice (horizontal axis; $n = 6$–8 mice). *, $P < 0.01$, versus wild-type mice; **, $P < 0.01$, versus GlcNAc6ST-1-deficient mice; ***, $P < 0.01$, versus GlcNAc6ST-2-deficient mice. **(f)** Trafficking of CMFDA-labeled lymphocytes to the inguinal lymph nodes of DNFB-sensitized mice (horizontal axis; $n = 3$ mice). *, $P < 0.01$, versus wild-type mice. Data (**a–d,f**) are representative of three independent experiments.

with L-sel–IgM were not detected in the ears of wild-type or mutant mice after the challenge (data not shown), suggesting that the reduction in the contact hypersensitivity response in double-knockout mice could have been due to qualitative or quantitative differences in the immune responses in the draining lymph nodes. *In vitro* proliferation of lymphocytes in response to the mitogen concanavalin A or to the water-soluble analog of DNFB, DNBS (2,4-dinitrobenzene sulfonic acid)[25], was almost indistinguishable in wild-type versus mutant mice (**Fig. 4c,d**). These data indicate that antigen-specific lymphocytes were present at almost the same ratio in the draining lymph nodes of both mouse lines. Notably, however, the total number of lymphocytes decreased by 70% in double-knockout mice (**Fig. 4e**). Consistent with that observation, lymphocyte trafficking to the draining lymph nodes significantly decreased in double-knockout mice in a short-term homing assay (**Fig. 4f**). These results collectively suggest that the reduced contact hypersensitivity response of double-knockout mice could be attributed to the quantitative decrease in the total number of antigen-specific lymphocytes recruited to the draining lymph nodes.

Carbohydrate structural analysis of GlyCAM-1

To gain insight into the structural basis of the substantial reduction in lymphocyte homing in the normal and pathophysiological conditions described above, we undertook carbohydrate structural analysis of GlyCAM-1. We first radiolabeled lymph nodes from wild-type and mutant mice with [^{3}H]galactose in organ culture and then released the *O*-glycans on GlyCAM-1 and did structural analysis. After removing sialic acid by mild acid hydrolysis, we fractionated oligosaccharides by gel filtration and anion-exchange column chromatography (**Supplementary Fig. 1** online). We then analyzed unsulfated oligosaccharides by exoglycosidase treatment and gel filtration. The amount of unsulfated oligosaccharides, including those containing the sialyl Lewis X structure, was substantially increased in double-knockout mice (**Fig. 5a**). We also analyzed sulfated oligosaccharide fractions in detail by exoglycosidase treatment and high-performance liquid chromatography (HPLC; **Supplementary Fig. 2** online). We found only very little oligosaccharide containing GlcNAc-6-*O*-sulfate in double-knockout mice (**Fig. 5a**). Conversely, the relative amount of sulfated oligosaccharides containing galactose-6-*O*-sulfate increased considerably in double-knockout mice (*O*-glycan structures, **Supplementary Fig. 3** online).

We calculated the amount of sialylated oligosaccharides from the amount of [^{3}H]galactose released by treatment of the total oligosaccharide fraction with a mixture of β-galactosidase and α-(1,3)- and α-(1,4)-fucosidase before and after the removal of sialic acid

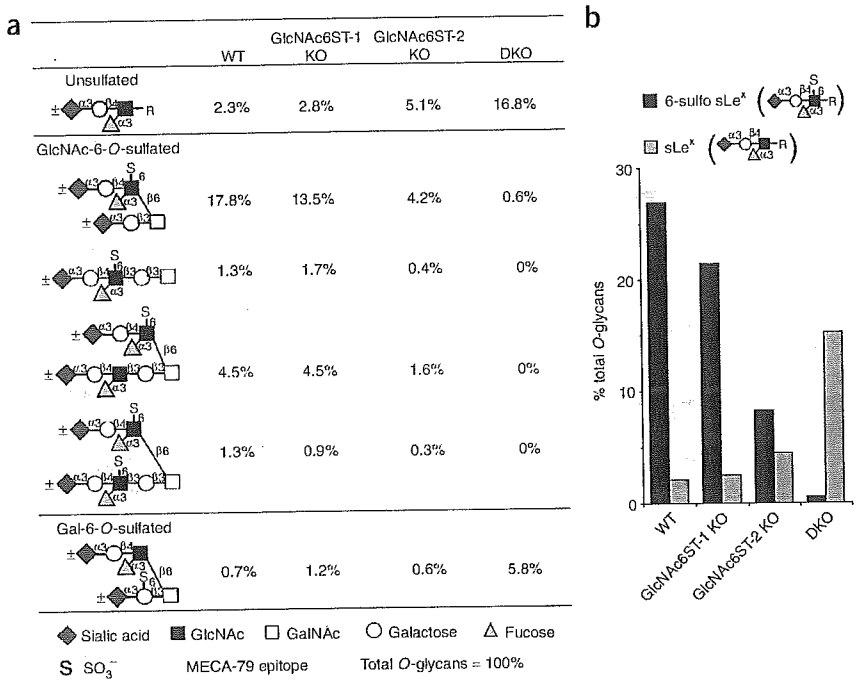

Figure 5 Structures of *O*-glycans attached to GlyCAM-1. (**a**) Fucosylated and/or sulfated *O*-glycans attached to GlyCAM-1 from wild-type and null mice. (**b**) Percentage of *O*-glycans attached to GlyCAM-1 containing 6-sulfo sialyl Lewis X (6-sulfo sLe^x) and unsulfated sialyl Lewis X (sLe^x). Total *O*-glycans attached to GlyCAM-1 = 100%. Data are representative of two independent experiments.

(**Supplementary Fig. 1** online). Sialic acid modification was present at the termini of 89.5%, 87.2%, 87.5% and 90.5% of the oligosaccharides in wild-type, GlcNAc6ST-1-deficient, GlcNAc6ST-2-deficient and double-knockout mice, respectively. Combined with the detailed structural analysis of the desialylated oligosaccharides, these results indicate that the 6-sulfo sialyl Lewis X structure was almost completely abrogated, whereas unsulfated sialyl Lewis X was overexpressed in the double-knockout mice (**Fig. 5b**).

Expression and substrate specificity of sulfotransferases

As shown above, some sulfated *O*-glycans were expressed in double-knockout mice. To determine which sulfotransferases were expressed and were involved in the biosynthesis of sulfated *O*-glycans in HEVs, we next did RT-PCR analysis using total RNA from peripheral lymph node HEV cells of wild-type mice, prepared by immunomagnetic selection with MECA-79 (**Fig. 6a**). After confirming expression of GlyCAM-1 and lack of expression of L-selectin in the MECA-79$^+$ HEV cell preparations, we examined the expression of sulfotransferases in these cell preparations. In addition to GlcNAc6ST-1 and GlcNAc6ST-2, we detected GlcNAc6ST-4 (refs. 26,27). Expression of GlcNAc6ST-3 (ref. 28) was not detectable in these cell preparations, although it was readily detectable in the same conditions in mouse cornea, which is known to express this sulfotransferase[29]. All four mouse GlcNAc6STs efficiently transferred sulfate to core 2–branched *O*-glycans, as shown by [^{35}S]Na_2SO_4 incorporation. In contrast, only GlcNAc6ST-2 and GlcNAc6ST-3 efficiently transferred sulfate to extended core 1 *O*-glycans, resulting in the generation of substantial MECA-79 epitope, as shown by immunoblot (**Fig. 6b**). GlcNAc6ST-1 inefficiently synthesized the MECA-79 epitope, whereas GlcNAc6ST-4 did not synthesize detectable amounts of this epitope, consistent with the finding that the MECA-79 epitope was abolished in the double-knockout mice (**Fig. 2a**). These results combined suggest that the small amount of core 2–branched *O*-glycans containing GlcNAc-6-*O*-sulfate identified in the double-knockout mice were synthesized by GlcNAc6ST-4. We also detected by RT-PCR expression of the galactose-6-*O*-sulfotransferase keratan sulfate sulfotransferase (KSST)[30], which is probably involved in the biosynthesis of the *O*-glycans containing galactose-6-*O*-sulfate identified in our carbohydrate analysis.

Functions of unsulfated sialyl Lewis X

As described above, the main carbohydrate structural changes in the double-knockout mice were the almost complete absence of the 6-sulfo sialyl Lewis X structure and abundant expression of the unsulfated sialyl Lewis X structure. To determine whether the low but detectable L-selectin ligand activity in the double-knockout mice was mediated by the unsulfated sialyl Lewis X structure, we assessed L-sel–IgM binding (**Fig. 6c**). Staining of L-sel–IgM on HEVs was abrogated in frozen sections of peripheral lymph nodes from mice doubly deficient in both FucT-IV and FucT-VII, indicating that fucose modification was critically important for binding of L-sel–IgM to the HEVs of peripheral lymph nodes. In addition, binding of L-sel–IgM to HEVs was abolished by sialidase treatment of frozen sections of peripheral lymph nodes from double-knockout mice, indicating that sialic acid modification was also indispensable. In accordance with those observations, preinjection of the fucose-specific lectin *Aleuria aurantia* agglutinin (AAA), or the α(2,3)-linked sialic acid–specific lectin *Maackia amurensis* agglutinin (MAA) into double-knockout mice inhibited homing of lymphocytes to peripheral lymph nodes by 85.2% or 78.7%, respectively (**Fig. 6d**). These results suggest that the residual L-selectin ligand activity in double-knockout mice was most likely mediated by the abundantly expressed unsulfated sialyl Lewis X structure.

DISCUSSION

We have shown here that GlcNAc6ST-1 and GlcNAc6ST-2 cooperatively have a chief function in the biosynthesis of L-selectin ligand carbohydrates in HEVs. Mutant mice deficient in both sulfotransferases showed substantially lower lymphocyte trafficking to peripheral lymph nodes, as well as less robust inflammatory responses after sensitization and challenge with the hapten DNFB. We also did a systematic carbohydrate structural analysis of a HEV-derived glycoprotein and have provided a structural 'explanation' for the phenotypes of mutant mice.

We have shown here that more than 25% of the total carbohydrates on GlyCAM-1 are modified with the 6-sulfo sialyl Lewis X capping structure on HEVs in wild-type mice, indicating that this carbohydrate structure is indeed a principal capping structure of GlyCAM-1. Carbohydrate structural analysis of double-knockout mice indicated that GlcNAc6ST-1 and GlcNAc6ST-2 are required for biosynthesis of this capping structure. Although we detected another member of the GlcNAc-6-*O*-sulfotransferase family, GlcNAc6ST-4, in MECA-79$^+$ HEV cells, structural analysis indicated

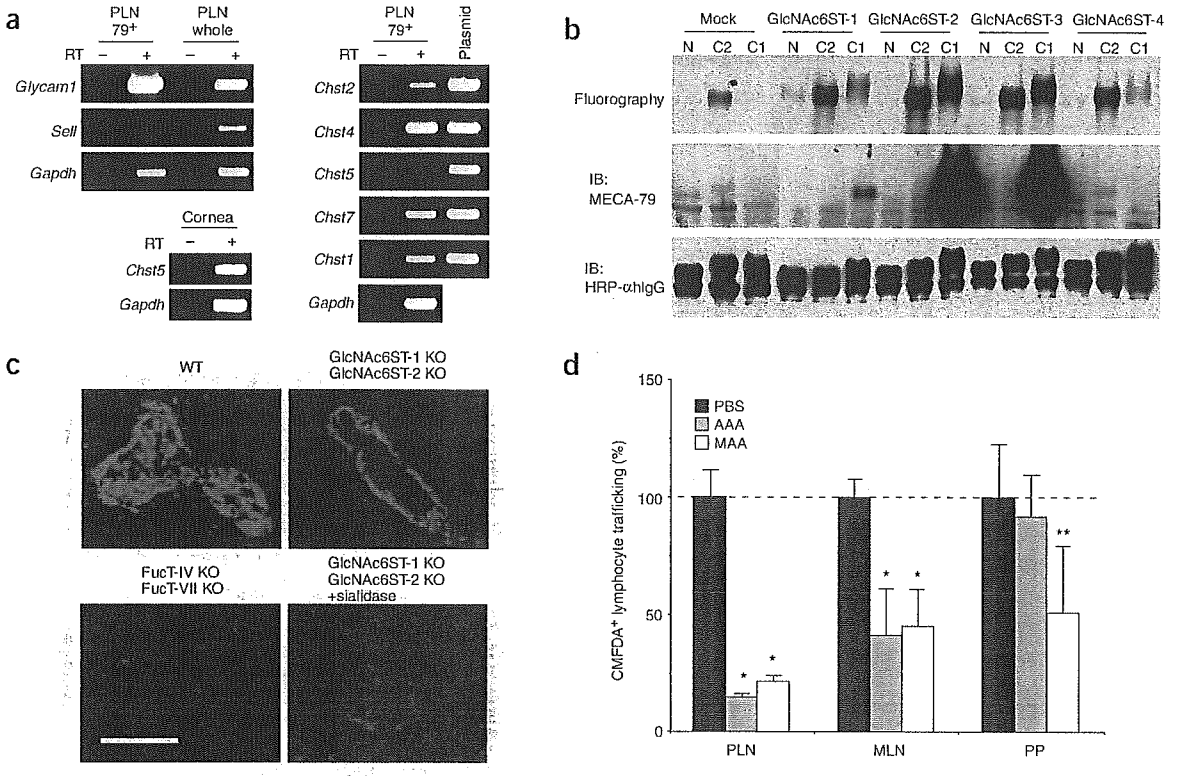

Figure 6 Expression of sulfotransferases in HEVs and characterization of remaining lymphocyte homing in double-knockout mice. **(a)** Expression of sulfotransferase genes. For this PCR, templates were single-stranded cDNAs constructed from MECA-79$^+$ HEVs from peripheral lymph nodes (PLN 79$^+$), whole-cell suspensions from peripheral lymph nodes (PLN whole) or corneas from wild-type mice (Cornea) or plasmid DNA containing full-length sulfotransferase cDNA (Plasmid). PCR was done in the presence (+) or absence (–) of reverse transcriptase (RT). *Chst2*, GlcNAc6ST-1; *Chst4*, GlcNAc6ST-2; *Chst5*, GlcNAc6ST-3; *Chst7*, GlcNAc6ST-4; *Chst1*, KSST; *Glycam1*, GlyCAM-1; *Sell*, L-selectin; *Gapdh*, glyceraldehyde-3-phosphate dehydrogenase. **(b)** Immunoblot of MECA-79. Lec2 cells were transiently transfected with expression vectors encoding GlyCAM-1-IgG without (N) or with Core2GlcNAcT-I (C2) and Core1-β3GlcNAcT (C1), together with nothing else (Mock) or with GlcNAc6ST-1–GlcNAc6ST-4. Cells were metabolically labeled with [^{35}S]Na_2SO_4. GlyCAM-1-IgG was purified with protein A–Sepharose and was analyzed by fluorography and immunoblot (IB) with MECA-79. The amount of GlyCAM-1-IgG was normalized by immunoblot with horseradish peroxidase–labeled antibody to human IgG (HRP-αhIgG). **(c)** Expression of L-selectin ligands. Frozen sections (7 μm in thickness) of peripheral lymph nodes from wild-type and mutant mice pretreated with sialidase (from *Vibrio cholerae*; 200 mU/ml) or not pretreated and stained with L-sel–IgM. Scale bar, 50 μm. **(d)** Trafficking of lymphocytes to lymphoid organs of double-knockout mice. CMFDA-labeled lymphocytes were injected into double-knockout mice 1 h after injection of phosphate-buffered saline (PBS), AAA lectin (100 μg) in PBS, or MAA lectin (40 μg) in PBS. Trafficking is presented as a percentage of that in PBS-injected mice, which was set as 100% ($n = 3$). *, $P < 0.01$, and **, $P < 0.1$, versus PBS-injected mice. Data are representative of three independent experiments.

that it has only a minor function in GlcNAc-6-*O*-sulfation of L-selectin ligands.

Although both GlcNAc6ST-1 and GlcNAc6ST-2 function in the GlcNAc-6-*O*-sulfation of L-selectin ligands, these sulfotransferases showed some differences in relation to L-selectin ligand biosynthesis in HEVs. GlcNAc6ST-2 seemed to be the main GlcNAc-6-*O*-sulfotransferase in peripheral lymph nodes and mesenteric lymph nodes, as staining with MECA-79 and L-sel–IgM binding was greatly diminished in the HEVs of these secondary lymphoid organs in the absence of GlcNAc6ST-2 but not in the absence of GlcNAc6ST-1. Consequently, homing of lymphocytes to these secondary lymphoid organs and the production of 6-sulfo sialyl Lewis X-containing *O*-glycans were more diminished in GlcNAc6ST-2-deficient mice than in GlcNAc6ST-1-deficient mice. Consistent with that finding, GlcNAc6ST-2 was expressed more abundantly in HEVs of peripheral lymph nodes than was GlcNAc6ST-1, as assessed by RT-PCR. In contrast, GlcNAc6ST-1 seemed to be the main GlcNAc-6-*O*-sulfotransferase in Peyer's patches, as MECA-79 antibody staining was abrogated in the absence of GlcNAc6ST-1. In accordance with that result, we found that expression of GlcNAc6ST-2 in Peyer's patches was undetectable, as judged by the fluorescence of the GlcNAc6ST-2–EGFP chimeric protein expressed under control of the promoter of the gene encoding GlcNAc6ST-2 (ref. 17).

Furthermore, GlcNAc6ST-2 seemed to be more relevant in the biosynthesis of fucosylated and sulfated *O*-glycans than GlcNAc6ST-1, because in mice deficient in GlcNAc6ST-2 alone, the percentage of *O*-glycans containing both fucose and sulfate was much lower, whereas the percentage of *O*-glycans containing only GlcNAc-6-*O*-sulfate but not fucose was slightly higher. The different ability in forming fucosylated and sulfated products may be due to the difference in the subcellular localizations of GlcNAc6ST-1 and GlcNAc6ST-2. GlcNAc6ST-1 is confined to the *trans*-Golgi network, whereas GlcNAc6ST-2 is distributed throughout the Golgi apparatus[31]; the latter may be more suitable to supply sulfated *O*-glycan acceptors to FucT-VII, a broadly Golgi-distributed glycosyltransferase[32], although further experimental verification is required to clarify that point.

Moreover, the acceptor substrate specificity of GlcNAc6ST-1 and GlcNAc6ST-2 overlaps but differs. Both sulfotransferases efficiently

transferred sulfate to core 2 *O*-glycans, whereas only GlcNAc6ST-2 efficiently transferred sulfate to extended core 1 *O*-glycans to form the MECA-79 epitope. These results collectively indicate that GlcNAc6ST-2 alone is not sufficient for full formation of 6-sulfo sialyl Lewis X despite its robust expression in HEVs of peripheral lymph nodes. The difference in the substrate specificities and possibly different subcellular localizations of GlcNAc6ST-1 and GlcNAc6ST-2 may contribute to the cooperative actions of these two sulfotransferases in the biosynthesis of L-selectin ligands in HEVs.

The homing of lymphocytes to peripheral lymph nodes in double-knockout mice was almost completely blocked by MEL-14. Although we detected binding of L-sel–IgM only on the lining of HEVs on the surface away from the lumen in double-knockout mice, it is conceivable that L-selectin ligands are weakly expressed on the lumenal surface of HEVs but below the detection level of immunofluorescence. The most likely candidate for supporting residual lymphocyte trafficking to peripheral lymph nodes in double-knockout mice is the unsulfated sialyl Lewis X structure, as it is abundantly expressed in the double-knockout mice and interacts with L-selectin *in vitro*[33]. In agreement with that hypothesis, homing of lymphocytes to peripheral lymph nodes is abolished in mice doubly deficient in both FucT-IV and FucT-VII (ref. 8). Similarly, our immunofluorescence study showed that L-sel–IgM did not bind to lymph node tissue sections of mice doubly deficient in both FucT-IV and FucT-VII. Moreover, preinjection of the fucose- and sialic acid–specific lectins AAA and MAA, respectively, inhibited homing of lymphocytes to peripheral lymph nodes and mesenteric lymph nodes in the double-knockout mice, indicating that both fucose and sialic acid are essential for residual lymphocyte homing in these mice.

Unsulfated sialyl Lewis X structures on extended core 1 as well as core 2–branched *O*-glycans efficiently support L-selectin-mediated lymphocyte rolling when the structures are present on P-selectin glycoprotein ligand 1, which contains sulfated tyrosine residues[34]. It has been reported that the P-selectin glycoprotein ligand 1–like molecule endoglycan, which is modified with the sialyl Lewis X structure and sulfated tyrosine residues, interacts efficiently with L-selectin[35]. It is possible, therefore, that the unsulfated sialyl Lewis X structure expressed in double-knockout mice supports lymphocyte rolling only when it is present on specific glycoproteins, such as endoglycan. However, our results have shown that GlyCAM-1 from double-knockout mice, which lacks tyrosine sulfation, weakly supported lymphocyte rolling, suggesting that abundant expression of unsulfated sialyl Lewis X in double-knockout mice may account at least in part for the residual lymphocyte homing. Indeed, GlyCAM-1 from double-knockout mice supported shear stress–dependent lymphocyte rolling, as expected given the L-selectin-dependent lymphocyte rolling[36]. The number of rolling lymphocytes on GlyCAM-1 from double-knockout mice decreased more than the number of lymphocytes with transient tethers. These results suggest that the rolling velocity is more affected than the initial tethering in double-knockout mice, consistent with the finding that 6-sulfation of sialyl Lewis X substantially decreases the rolling velocity of lymphocytes[13,17,37]. Intravital microscopy has shown the rolling velocity of lymphocytes increases considerably in the double-knockout mice, which results in a substantial reduction in the number of cells sticking on HEVs[38]. That same analysis has also shown that the rolling of B lymphocytes is diminished more substantially in HEVs than in medullary venules, consistent with the finding that rolling in HEVs is more dependent on sulfation than is rolling in medullary venules, as assessed by MECA-79 antigen expression[39]. Along with our carbohydrate structural analysis, those studies suggest that sialyl Lewis X can function as a substitute L-selectin ligand in the absence of 6-sulfo sialyl Lewis X, although the rolling velocity supported by the former is much faster than that supported by the latter.

In addition to the abundant unsulfated sialyl Lewis X in double-knockout mice, we have identified a previously unknown structure containing unsulfated sialyl Lewis X in the core 2 branch and galactose-6-*O*-sulfate in the core 1 branch; this carbohydrate structure represented 5.8% of the total carbohydrates on GlyCAM-1 derived from double-knockout mice. It is possible that this structure is also partially responsible for residual L-selectin ligand activity in these mice, as transfection of cDNA encoding KSST enhances L-selectin ligand activity *in vitro*[14,37]. However, this structure should have minimal involvement in lymphocyte homing, because the substantial increase in its abundance in double-knockout mice was not associated with an increase in lymphocyte homing activity.

Although it has been reported that the 6′-sulfo sialyl Lewis X capping structure (sialyl-α(2-3)-[sulfo-6]-galactopyranosyl-β(1-4)-[fucopyranosyl-α(1-3)]-*N*-acetylglucosaminyl-β1-R) is expressed in HEVs[40], we did not detect this carbohydrate structure in our analysis, possibly because this structure is not efficiently synthesized because of acceptor competition between FucT-VII and KSST. As described before, FucT-VII transfers few if any fucose residues to sialyl lactosamine modified with galactose-6-*O*-sulfate[7]. Conversely, KSST does not transfer sulfate to the galactose residue of the sialyl Lewis X structure[41]. Combined with our carbohydrate analysis, those findings suggest that KSST overexpression may negatively regulate L-selectin ligand activity by competing for acceptor substrates with FucT-VII, as fucosylation by FucT-VII is critically important for the biosynthesis of L-selectin ligands[7]. Preliminary results have indicated that KSST overexpression indeed inhibits sialyl Lewis X expression in FucT-VII transfectants (N.H., H.K. and M.F., unpublished observations). Thus, KSST may function both positively[14,37] and negatively in the biosynthesis of L-selectin ligand carbohydrates, depending on its abundance.

To determine the functions of GlcNAc6ST-1 and GlcNAc6ST-2 in immune responses in pathophysiological conditions, we assessed contact hypersensitivity responses in double-knockout mice and found that these mice had substantially less in ear swelling and leukocyte infiltration than did wild-type mice. We also found that the total number of lymphocytes was greatly reduced in the draining lymph nodes after sensitization with DNFB, although antigen-specific lymphocytes were present in the draining lymph nodes at the same ratio found in wild-type mice. Thus, it is likely that the quantitative reduction in antigen-specific lymphocytes resulted in the overall reduction in the contact hypersensitivity responses in these mice. This reduction occurred only in the double-knockout mice, indicating a critical threshold for the amount of L-selectin ligands to attain normal contact hypersensitivity responses. Our results are reminiscent of the phenotypes of L-selectin-deficient mice[42] and mice doubly deficient in both FucT-IV and FucT-VII (ref. 43), in which contact hypersensitivity responses are impaired due in part to a lack of antigen-specific lymphocytes in the draining lymph nodes. In mice deficient in L-selectin or fucosyltransferase, however, not only homing of naive lymphocytes to the regional lymph nodes but also effector cell trafficking to the inflammatory sites is impaired, because the interaction between L-selectin and sialyl Lewis X–modified P-selectin glycoprotein ligand 1 is completely abolished. In contrast, only the former was impaired in our sulfotransferase double-knockout mice. Thus, we have shown that homing of naive lymphocytes to the regional lymph nodes is actually a key determinant of the contact hypersensitivity response.

HEV-like vessels reactive with MECA-79 are detected in several disorders associated with chronic inflammation[44]. MECA-79-reactive

HEV-like vessels are detected in human gastric mucosa infected by *Helicobacter pylori*[45]. However, the physiological function of the MECA-79 epitope expressed in these specialized blood vessels is unclear, except for the demonstration that MECA-79 has a therapeutic effect in a sheep model of asthma[46]. As double-knockout mice completely lack the MECA-79 epitope, these mice will be useful for assessing the functions of this carbohydrate epitope at sites of chronic inflammation, such as the pancreas and salivary glands of nonobese diabetic mice[47,48], the hyperplastic thymus of AKR mice[49], the inflamed joints of rheumatoid arthritis[50] and the mouse model for inflammation induced by *H. pylori (felis)*[51].

In conclusion, our findings have demonstrated the essential function of GlcNAc6ST-1 and GlcNAc6ST-2 in the biosynthesis of the 6-sulfo sialyl Lewis X structure in HEVs, which serves as a dominant ligand for the lymphocyte-homing receptor L-selectin. Our studies provide a link between carbohydrate structural changes and alterations in trafficking of lymphocytes to secondary lymphoid organs in normal and pathophysiological conditions. As many studies have linked carbohydrates to immune cell recruitment, studies linking carbohydrate structure and function should become increasingly important in this field.

METHODS

Mice. Double-knockout mice were generated by breeding of mice singly deficient in GlcNAc6ST-1 (ref. 23) and GlcNAc6ST-2 (ref. 17). Genomic DNA was isolated from mouse tails and was used for PCR genotyping. For the simultaneous detection of wild-type and mutant alleles encoding GlcNAc6ST-1, primers 5′-TCTATGAGCCTGTGTGGCACGT-3′ (G6W5), 5′-GCATACCACCTTGTTAGTGGC-3′ (G6W3) and 5′-TGACAACGTCGAG CACAGCTG-3′ (NeoP5) were used. For detection of the alleles encoding GlcNAc6ST-2, primers F2W, R2W and R1M were used as described[17]. Mice doubly deficient in both FucT-IV and FucT-VII, generated as described[8], were provided by the Functional Glycomics Consortium (La Jolla, California). Mice were treated in accordance with guidelines of the National Institutes of Health and the United States Department of Agriculture and experiments were approved by the Animal Research Committee of the Burnham Institute (La Jolla, California).

Lymphocyte homing assay. This was done as described[17]. Lymphocytes from spleens and mesenteric lymph nodes of wild-type mice were labeled with chloromethyl fluorescence diacetate (CMFDA) and 2.5×10^7 cells were injected into the tail veins of 7- to 8-week-old wild-type and mutant mice. After 1 h, mice were killed and peripheral lymph nodes, mesenteric lymph nodes and Peyer's patches were collected. Lymphocyte suspensions were prepared from these organs and were analyzed by flow cytometry to determine the fractional content of fluorescent cells.

Lymphocyte rolling assay. GlyCAM-1 was purified from serum obtained from mice of each strain[52]. The concentration of GlyCAM-1 in each preparation was almost equivalent, as assessed by immunoblot with antibody to GlyCAM-1 prepared in a similar way as described[52]. Purified GlyCAM-1 (10 μl; equivalent to the amount of GlyCAM-1 purified from 10 μl of serum) was applied twice (6 h and overnight) or three times (6 h, overnight, and 6 h) in parallel to polystyrene plates coated with antibody to GlyCAM-1 at concentrations of 20 or 50 μg/ml, respectively. Lymphocytes were added to the flow chamber and were analyzed as described[8]. Based on velocity, rolling cells were classified into two groups: rolling lymphocytes that rolled at least two cell diameters for more than 0.5 s below critical velocity, and transiently tethered lymphocytes that had a high rolling velocity near that of free-floating cells with multiple pauses in less than 0.5 s.

Contact hypersensitivity. Contact hypersensitivity responses were measured as described[25]. The dorsal skin of mice was shaved and 25 μl of 0.5% DNFB (Sigma) in acetone/olive oil (4:1, volume/volume) was applied on days 0 and 1. On day 5, the right ear was treated with 20 μl of 0.2% DNFB (10 μl on the side of the pinna) and the left ear was treated with vehicle. Swelling was measured with a thickness gauge before and 24 h after treatment.

Lymphocyte proliferation assay. Single-cell suspensions were prepared from inguinal lymph nodes of mice sensitized with DNFB on days 0 and 1 as described above and were cultured for 40 h in the presence or absence of 2 μg/ml of concanavalin A (Sigma) or 200 μg/ml of DNBS[25] (MP Biomedicals). Cell proliferation was measured with a CellTiter 96AQueous One Solution Proliferation Assay kit (Promega). The absorbance at 490 nm obtained in the absence of concanavalin A or DNBS was subtracted from that obtained in the presence of these agents.

Structural analysis of *O*-glycans attached to GlyCAM-1. Peripheral lymph node and mesenteric lymph node slices were metabolically labeled with 0.5 mCi/ml of [^{3}H]galactose (American Radiolabeled Chemicals) as described[15,17]. GlyCAM-1 was purified from the conditioned medium and its *O*-glycans were analyzed by Bio-Gel P-4 gel filtration (Bio-Rad), QAE-Sephadex A-25 anion-exchange column (Sigma) and HPLC before and after exoglycosidase treatment, as described[13,15,17], except that the elution condition of the Asahipak NH_2-bonded HPLC column was modified. Solvent A (64% acetonitrile and 36% H_2O), solvent B (25 mM NaH_2PO_4 in solvent A) and solvent C (50 mM NaH_2PO_4 in solvent A) were used for HPLC as follows. Monosulfated tetrasaccharide core *O*-glycans were eluted with a linear gradient from 0% to 30% solvent B in solvent A for 10 min; from 30% to 65% for 40 min; and from 65% to 100% for 5 min, followed by 100% solvent B for 5 min. Monosulfated hexasaccharide core *O*-glycans were eluted with a linear gradient from 0% to 40% solvent B in solvent A for 10 min; from 40% to 80% for 40 min; and from 80% to 100% for 5 min, followed by 100% solvent B for 5 min. Disulfated *O*-glycans were eluted with a linear gradient from 0% to 40% solvent C in solvent A for 10 min; from 40% to 80% for 40 min; and from 80% to 100% for 5 min, followed by 100% solvent C for 15 min.

RT-PCR. HEV cells were purified from peripheral lymph nodes of C57BL/6 mice by immunomagnetic selection with MECA-79 (ref. 53). Mouse corneas were excised surgically from C57BL/6 mice. Total RNA was purified from these preparations and was used for RT-PCR as described[13]. Primers used to detect genes encoding mouse GlcNAc6ST-1 and mouse GlcNAc6ST-2 have been described[13]. Primers used to detect genes encoding other molecules were as follows: 5′-TGCTGGTACTGTCCTCGTGG-3′ and 5′-TGATGTTGCCACGAGC GAAGG-3′ for mouse GlcNAc6ST-3; 5′-TCAACCTAAAGGTGGTGCAACT-3′ and 5′-GGTTAAGAAGAAATCAGCGCGT-3′ for mouse GlcNAc6ST-4; 5′-AAG CCCTACAACCTGGATGTG-3′ and 5′-GAGTTGCGCACTGTGCTGTAT-3′ for mouse KSST; 5′-CGGAATTCCCACCATGAAATTCTTCAC-3′ and 5′-CGGGAT CCAGTTCTTCCTCCACTGTC-3′ for mouse GlyCAM-1; 5′-CTCTGCTACA CAGCCTCTTGC-3′ and 5′-AGGCTCACACTGGACCACTTG-3′ for mouse L-selectin; and 5′-CCTGGCCAAGGTCATCCATGACA-3′ and 5′-ATGAGGTCC ACCACCCTGTTGCT-3′ for mouse glyceraldehyde-3-phosphate dehydrogenase.

Transient transfection and metabolic cell labeling. Lec2 cells[54] were transiently transfected with an expression plasmid encoding GlyCAM-1–IgG[13] in combination with those encoding core 2–*N*-acetylglucosaminyltransferase-I (Core2GlcNAcT-I) or core 1–β1,3-*N*-acetylglucosaminyltransferase (Core1-β3GlcNAcT) and one of the four GlcNAc6STs (GlcNAc6ST-1 through GlcNAc6ST-4). Cells were metabolically labeled with [^{35}S]Na_2SO_4 (100 μCi/ml) as described[13,15]. As a control, vectors without inserts were transfected into Lec2 cells. In Lec2 cells, MECA-79 antigen is efficiently synthesized, as Lec2 cells lack Golgi-sialylation[54] and thus core 1 extension does not compete with α2,3-sialylation of core 1 structure (galactopyranosyl-β(1-3)-*N*-acetylgalactosaminyl-α1-serine (or threonine)).

Statistical analysis. Student's *t*-test was used for statistical analysis.

Accession code. BIND (http://bind.ca): 319185.

Note: Supplementary information is available on the Nature Immunology website.

ACKNOWLEDGMENTS

We thank T. Akama, S. Chen and E. Lammar for critical reading of the manuscript, and A. Morse for organizing the manuscript. Supported by the

National Institutes of Health (P01CA71932 to M.F. and J.B.L.; U54 GM62116 to the Functional Glycomics Consortium) and the Uehara Memorial Foundation, Japan (H.K.).

COMPETING INTERESTS STATEMENT
The authors declare that they have no competing financial interests.

Published online at http://www.nature.com/natureimmunology/
Reprints and permissions information is available online at http://npg.nature.com/reprintsandpermissions/

1. Arbonés, M.L. *et al.* Lymphocyte homing and leukocyte rolling and migration are impaired in L-selectin-deficient mice. *Immunity* **1**, 247–260 (1994).
2. Springer, T.A. Traffic signals for lymphocyte recirculation and leukocyte emigration: the multistep paradigm. *Cell* **76**, 301–314 (1994).
3. Butcher, E.C. & Picker, L.J. Lymphocyte homing and homeostasis. *Science* **272**, 60–66 (1996).
4. von Andrian, U.H. & Mempel, T.R. Homing and cellular traffic in lymph nodes. *Nat. Rev. Immunol.* **3**, 867–878 (2003).
5. Ley, K. & Kansas, G.S. Selectins in T-cell recruitment to non-lymphoid tissues and sites of inflammation. *Nat. Rev. Immunol.* **4**, 325–335 (2004).
6. Rosen, S.D. Ligands for L-selectin: homing, inflammation, and beyond. *Annu. Rev. Immunol.* **22**, 129–156 (2004).
7. Maly, P. *et al.* The α(1,3)fucosyltransferase Fuc-TVII controls leukocyte trafficking through an essential role in L-, E-, and P-selectin ligand biosynthesis. *Cell* **86**, 643–653 (1996).
8. Homeister, J.W. *et al.* The α(1,3) fucosyltransferases FucT-IV and FucT-VII exert collaborative control over selectin-dependent leukocyte recruitment and lymphocyte homing. *Immunity* **15**, 115–126 (2001).
9. Rosen, S.D., Singer, M.S. & Yednock, T.A. Involvement of sialic acid on endothelial cells in organ-specific lymphocyte recirculation. *Science* **228**, 1005–1007 (1985).
10. Imai, Y., Lasky, L.A. & Rosen, S.D. Sulphation requirement for GlyCAM-1, an endothelial ligand for L-selectin. *Nature* **361**, 555–557 (1993).
11. Hemmerich, S., Butcher, E.C. & Rosen, S.D. Sulfation-dependent recognition of high endothelial venules (HEV)-ligands by L-selectin and MECA-79, an adhesion-blocking monoclonal antibody. *J. Exp. Med.* **180**, 2219–2226 (1994).
12. Mitsuoka, C. *et al.* Identification of a major carbohydrate capping group of the L-selectin ligand on high endothelial venules in human lymph nodes as 6-sulfo sialyl Lewis X. *J. Biol. Chem.* **273**, 11225–11233 (1998).
13. Hiraoka, N. *et al.* A novel, high endothelial venule-specific sulfotransferase expresses 6-sulfo sialyl Lewis^x, an L-selectin ligand displayed by CD34. *Immunity* **11**, 79–89 (1999).
14. Bistrup, A. *et al.* Sulfotransferases of two specificities function in the reconstitution of high endothelial cell ligands for L-selectin. *J. Cell Biol.* **145**, 899–910 (1999).
15. Yeh, J.-C. *et al.* Novel sulfated lymphocyte homing receptors and their control by a core1 extension β1,3-*N*-acetylglucosaminyltransferase. *Cell* **105**, 957–969 (2001).
16. Streeter, P.R., Rouse, B.T.N. & Butcher, E.C. Immunohistologic and functional characterization of a vascular addressin involved in lymphocyte homing into peripheral lymph nodes. *J. Cell Biol.* **107**, 1853–1862 (1988).
17. Hiraoka, N. *et al.* Core 2 branching β1,6-*N*-acetylglucosaminyltransferase and high endothelial venule-restricted sulfotransferase collaboratively control lymphocyte homing. *J. Biol. Chem.* **279**, 3058–3067 (2004).
18. Hemmerich, S. *et al.* Sulfation of L-selectin ligands by an HEV-restricted sulfotransferase regulates lymphocyte homing to lymph nodes. *Immunity* **15**, 237–247 (2001).
19. Fukuda, M., Hiraoka, N., Akama, T.O. & Fukuda, M.N. Carbohydrate-modifying sulfotransferases: structure, function and pathophysiology. *J. Biol. Chem.* **276**, 47747–47750 (2001).
20. Hemmerich, S. *et al.* Chromosomal localization and genomic organization for the galactose/*N*-acetylgalactosamine/*N*-acetylglucosamine 6-*O*-sulfotransferase gene family. *Glycobiology* **11**, 75–87 (2001).
21. Uchimura, K. *et al.* Molecular cloning and characterization of an *N*-acetylglucosamine-6-*O*-sulfotransferase. *J. Biol. Chem.* **273**, 22577–22583 (1998).
22. Kimura, N. *et al.* Reconstitution of functional L-selectin ligands on a cultured human endothelial cell line by cotransfection of α1–3 fucosyltransferase VII and newly cloned GlcNAcβ:6-sulfotransferase cDNA. *Proc. Natl. Acad. Sci. USA* **96**, 4530–4535 (1999).
23. Uchimura, K. *et al.* *N*-Acetylglucosamine 6-*O*-sulfotransferase-1 regulates expression of L-selectin ligands and lymphocyte homing. *J. Biol. Chem.* **279**, 35001–35008 (2004).
24. Berlin, C. *et al.* $\alpha_4\beta_7$ integrin mediates lymphocyte binding to the mucosal vascular addressin MAdCAM-1. *Cell* **74**, 185–195 (1993).
25. Phanuphak, P., Moorhead, J.W. & Claman, H.N. Tolerance and contact sensitivity to DNFB in mice. I. *In vivo* detection by ear swelling and correlation with *in vitro* cell stimulation. *J. Immunol.* **112**, 115–123 (1974).
26. Uchimura, K. *et al.* Diversity of *N*-acetylglucosamine-6-*O*-sulfotransferases: molecular cloning of a novel enzyme with different distribution and specificities. *Biochem. Biophys. Res. Commun.* **274**, 291–296 (2000).
27. Bhakta, S. *et al.* Sulfation of *N*-acetylglucosamine by chondroitin 6-sulfotransferase 2 (GST-5). *J. Biol. Chem.* **275**, 40226–40234 (2000).
28. Lee, J.K., Bhakta, S., Rosen, S.D. & Hemmerich, S. Cloning and characterization of a mammalian *N*-acetylglucosamine-6-sulfotransferase that is highly restricted to intestinal tissue. *Biochem. Biophys. Res. Commun.* **263**, 543–549 (1999).
29. Akama, T.O. *et al.* Human corneal GlcNAc 6-*O*-sulfotransferase and mouse intestinal GlcNAc 6-*O*-sulfotransferase both produce keratan sulfate. *J. Biol. Chem.* **276**, 16271–16278 (2001).
30. Fukuta, M. *et al.* Molecular cloning and characterization of human keratan sulfate Gal-6-sulfotransferase. *J. Biol. Chem.* **272**, 32321–32328 (1997).
31. de Graffenried, C.L. & Bertozzi, C.R. Golgi localization of carbohydrate sulfotransferases is a determinant of L-selectin ligand biosynthesis. *J. Biol. Chem.* **278**, 40282–40295 (2003).
32. Zerfaoui, M. *et al.* The cytosolic and transmembrane domains of the β1,6 *N*-acetylglucosaminyltransferase (C2GnT) function as a *cis* to *medial*/Golgi-targeting determinant. *Glycobiology* **12**, 15–24 (2002).
33. Foxall, C. *et al.* The three members of the selectin receptor family recognize a common carbohydrate epitope, the sialyl Lewis^x oligosaccharide. *J. Cell Biol.* **117**, 895–902 (1992).
34. Mitoma, J. *et al.* Extended core 1 and core 2 branched *O*-glycans differentially modulate sialyl Lewis x-type L-selectin ligand activity. *J. Biol. Chem.* **278**, 9953–9961 (2003).
35. Fieger, C.B., Sassetti, C.M. & Rosen, S.D. Endoglycan, a member of the CD34 family, functions as an L-selectin ligand through modification with tyrosine sulfation and sialyl Lewis x. *J. Biol. Chem.* **278**, 27390–27398 (2003).
36. Finger, E.B. *et al.* Adhesion through L-selectin requires a threshold hydrodynamic shear. *Nature* **379**, 266–269 (1996).
37. Tangemann, K., Bistrup, A., Hemmerich, S. & Rosen, S.D. Sulfation of a high endothelial venule-expressed ligand for L-selectin: effects on tethering and rolling of lymphocytes. *J. Exp. Med.* **190**, 935–941 (1999).
38. Uchimura, K. *et al.* A major class of L-selectin ligands is eliminated in mice deficient in two sulfotransferases expressed in high endothelial venules. *Nat. Immunol.* advance online publication 9 October 2005(doi:1038/ni 1258).
39. M'Rini, C. *et al.* A Novel endothelial L-selectin ligand activity in lymph node medulla that is regulated by α(1,3)-fucosyltransferase-IV. *J. Exp. Med.* **198**, 1301–1312 (2003).
40. Hemmerich, S., Leffler, H. & Rosen, S.D. Structure of the *O*-glycans in GlyCAM-1, an endothelial-derived ligand for L-selectin. *J. Biol. Chem.* **270**, 12035–12047 (1995).
41. Torii, T., Fukuta, M. & Habuchi, O. Sulfation of sialyl *N*-acetyllactosamine oligosaccharides and fetuin oligosaccharides by keratan sulfate Gal-6-sulfotransferase. *Glycobiology* **10**, 203–211 (2000).
42. Catalina, M.D. *et al.* The route of antigen entry determines the requirement for L-selectin during immune responses. *J. Exp. Med.* **184**, 2341–2351 (1996).
43. Smithson, G. *et al.* Fuc-TVII is required for T helper 1 and T cytotoxic 1 lymphocyte selectin ligand expression and recruitment in inflammation, and together with Fuc-TIV regulates naive T cell trafficking to lymph nodes. *J. Exp. Med.* **194**, 601–614 (2001).
44. Rosen, S.D. Endothelial ligands for L-selectin. From lymphocyte recirculation to allograft rejection. *Am. J. Pathol.* **155**, 1013–1020 (1999).
45. Kobayashi, M. *et al.* Induction of peripheral lymph node addressin in human gastric mucosa infected by *Helicobacter pylori*. *Proc. Natl. Acad. Sci. USA* **101**, 17807–17812 (2004).
46. Rosen, S.D., Tsay, D., Singer, M.S., Hemmerich, S. & Abraham, W.M. Therapeutic targeting of endothelial ligands for L-selectin (PNAd) in a sheep model of asthma. *Am. J. Pathol.* **166**, 935–944 (2005).
47. Hanninen, A. *et al.* Vascular addressins are induced on islet vessels during insulitis in nonobese diabetic mice and are involved in lymphoid cell binding to islet endothelium. *J. Clin. Invest.* **92**, 2509–2515 (1993).
48. Faveeuw, C., Gagnerault, M-C. & Lepault, F. Expression of homing and adhesion molecules in infiltrated islets of Langerhans and salivary glands of nonobese diabetic mice. *J. Immunol.* **152**, 5969–5978 (1994).
49. Michie, S.A., Streeter, P.R., Butcher, E.C. & Rouse, R.V. L-selectin and $\alpha_4\beta_7$ integrin homing receptor pathways mediate peripheral lymphocyte traffic to AKR mouse hyperplastic thymus. *Am. J. Pathol.* **147**, 412–421 (1995).
50. Michie, S.A., Streeter, P.R., Bolt, P.A., Butcher, E.C. & : Picker, L.J. The human peripheral lymph node vascular addressin. An inducible endothelial antigen involved in lymphocyte homing. *Am. J. Pathol.* **143**, 1688–1698 (1993).
51. Fox, J.G. *et al.* Hypertrophic gastropathy in *Helicobacter felis*-infected wild-type C57BL/6 mice and p53 hemizygous transgenic mice. *Gastroenterology* **110**, 155–166 (1996).
52. Singer, M.S. & Rosen, S.D. Purification and quantification of L-selectin-reactive GlyCAM-1 from mouse serum. *J. Immunol. Methods* **196**, 153–161 (1996).
53. Girard, J.P. & Springer, T.A. Cloning from purified high endothelial venule cells of hevin, a close relative of the antiadhesive extracellular matrix protein SPARC. *Immunity* **2**, 113–123 (1995).
54. Deutscher, S.L., Nuwayhid, N., Stanley, P., Briles, E.I. & Hirschberg, C.B. Translocation across Golgi vesicle membranes: a CHO glycosylation mutant deficient in CMP-sialic acid transport. *Cell* **39**, 295–299 (1984).

Enhancing transplant efficiency has clinical implication but is being debated. Recent reports suggest that HSCs engraft mice with absolute efficiency (*7*, *8*). One report (*7*) was heavily influenced by mathematical correction factors, and the other (*8*) addressed single-cell transplants by a subset of HSCs among competitor cells that themselves could save the lethally irradiated recipient. Contrary to this is the reality of the clinical situation (*3*) and studies in which injection of HSCs directly into BM showed enhanced engraftment compared with intravenous administering of cells (*29*–*31*). Removal of endogenous CD26 activity on donor HSCs increased homing and engraftment. Thus, improvement in transplant efficiency is possible. Further advancement may require more effective use of CD26 inhibitors, which may translate into the use of HSCs for clinical transplantation from sources containing limiting cell numbers, such as cord blood.

References and Notes

1. H. E. Broxmeyer *et al.*, *Proc. Natl. Acad. Sci. U.S.A.* **86**, 3828 (1989).
2. E. Gluckman *et al.*, *N. Engl. J. Med.* **321**, 1174 (1989).
3. H. E. Broxmeyer, F. Smith, in *Thomas' Hematopoietic Cell Transplantation*, K. G. Blume, S. J. Forman, F. R. Appelbaum, Eds. (Blackwell Science, Oxford; Malden, MA, 2004), chap. 43, pp. 550–564.
4. E. J. Shpall *et al.*, *Biol. Blood Marrow Transplant.* **8**, 368 (2002).
5. J. Jaroscak *et al.*, *Blood* **101**, 5061 (2003).
6. H. Ema, H. Nakauchi, *Immunity* **20**, 1 (2004).
7. P. Benveniste, C. Cantin, D. Hyam, N. N. Iscove, *Nature Immunol.* **4**, 708 (2003).
8. Y. Matsuzaki, K. Kinjo, R. C. Mulligan, H. Okano, *Immunity* **20**, 87 (2004).
9. K. W. Christopherson 2nd, G. Hangoc, H. E. Broxmeyer, *J. Immunol.* **169**, 7000 (2002).
10. K. W. Christopherson 2nd, S. Cooper, H. E. Broxmeyer, *Blood* **101**, 4680 (2003).
11. K. W. Christopherson 2nd, S. Cooper, G. Hangoc, H. E. Broxmeyer, *Exp. Hematol.* **31**, 1126 (2003).
12. G. J. Spangrude, S. Heimfeld, I. L. Weissman, *Science* **241**, 58 (1988).
13. D. E. Harrison, *Blood* **55**, 77 (1980).
14. Materials and methods are available as supporting material on *Science* Online.
15. M. M. Rosenkilde *et al.*, *J. Biol. Chem.* **279**, 3033 (2004).
16. D. E. Wright, E. P. Bowman, A. J. Wagers, E. C. Butcher, I. L. Weissman, *J. Exp. Med.* **195**, 1145 (2002).
17. K. Hattori *et al.*, *Blood* **97**, 3354 (2001).
18. H. E. Broxmeyer *et al.*, *Blood* **100**, 609a (abstr. no. 2397) (2002).
19. C. W. Liles *et al.*, *Blood* **102**, 2728 (2003).
20. A. Peled *et al.*, *Science* **283**, 845 (1999).
21. H. E. Broxmeyer, *Int. J. Hematol.* **74**, 9 (2001).
22. T. Ara *et al.*, *Immunity* **19**, 257 (2003).
23. C. H. Kim, H. E. Broxmeyer, *Blood* **91**, 100 (1998).
24. H. E. Broxmeyer *et al.*, *J. Immunol.* **170**, 421 (2003).
25. H. E. Broxmeyer *et al.*, *J. Leukoc. Biol.* **73**, 630 (2003).
26. O. Kollet *et al.*, *Blood* **100**, 2778 (2002).
27. D. E. Harrison, C. T. Jordan, R. K. Zhong, C. M. Astle, *Exp. Hematol.* **21**, 206 (1993).
28. A. Gothot, J. C. van der Loo, D. W. Clapp, E. F. Srour, *Blood* **92**, 2641 (1998).
29. T. Yahata *et al.*, *Blood* **101**, 2905 (2003).
30. J. Wang *et al.*, *Blood* **101**, 2924 (2003).
31. F. Mazurier, M. Doedens, O. I. Gan, J. E. Dick, *Nature Med.* **9**, 959 (2003).

32. These studies were supported by U.S. Public Health Science Grants R01 DK53674, R01 HL67384, and R01 HL56416 to H.E.B. K.W.C. was supported sequentially during these studies by NIH training grant T32 DK07519 to H.E.B. and by a Fellow Award from the Leukemia and Lymphoma Society to K.W.C.

Supporting Online Material

www.sciencemag.org/cgi/content/full/305/5686/1000/DC1

Materials and Methods

Figs. S1 to S5

References

23 February 2004; accepted 15 July 2004

Natural Antibiotic Function of a Human Gastric Mucin Against *Helicobacter pylori* Infection

Masatomo Kawakubo,[1,2] Yuki Ito,[1] Yukie Okimura,[2] Motohiro Kobayashi,[1,4] Kyoko Sakura,[2] Susumu Kasama,[1] Michiko N. Fukuda,[4] Minoru Fukuda,[4] Tsutomu Katsuyama,[2] Jun Nakayama[1,3]*

Helicobacter pylori infects the stomachs of nearly a half the human population, yet most infected individuals remain asymptomatic, which suggests that there is a host defense against this bacterium. Because *H. pylori* is rarely found in deeper portions of the gastric mucosa, where *O*-glycans are expressed that have terminal α1,4-linked *N*-acetylglucosamine, we tested whether these *O*-glycans might affect *H. pylori* growth. Here, we report that these *O*-glycans have antimicrobial activity against *H. pylori*, inhibiting its biosynthesis of cholesteryl-α-D-glucopyranoside, a major cell wall component. Thus, the unique *O*-glycans in gastric mucin appeared to function as a natural antibiotic, protecting the host from *H. pylori* infection.

Helicobacter pylori colonizes the gastric mucosa of about half the world's population and is considered a leading cause of gastric malignancies (*1*–*3*). However, most infected individuals remain asymptomatic or are affected merely by chronic active gastritis (*2*). Only a fraction of infected patients develop peptic ulcer, gastric cancer, and malignant lymphoma. This suggests the presence of host defense mechanisms against *H. pylori* pathogenesis.

Gastric mucins are classified into two types based on their histochemical properties (*4*). The first is a surface mucous cell–type mucin, secreted from the surface mucous cells. The second is found in deeper portions of the mucosa and is secreted by gland mucous cells, including mucous neck cells, cardiac gland cells, and pyloric gland cells.

In *H. pylori* infection, the bacteria are associated solely with surface mucous cell–type mucin (*5*), and two carbohydrate structures, Lewis b and sialyl dimeric Lewis X in surface mucous cells, serve as specific ligands for *H. pylori* adhesins, BabA and SabA, respectively (*6*, *7*). *H. pylori* rarely colonizes the deeper portions of gastric mucosa, where the gland mucous cells produce mucins having terminal α1,4-linked *N*-acetylglucosamine (α1,4-GlcNAc) residues attached to core 2–branched *O*-glycans [GlcNAcα1→4Galβ1→4GlcNAcβ1→6(GlcNAcα1→ 4Galβ1→3)GalNAcα→Ser/Thr] (*8*). Development of pyloric gland atrophy enhances the risk of peptic ulcer or gastric cancer two- to three-fold compared with chronic gastritis without pyloric gland atrophy (*3*). These findings raise the possibility that α1,4-GlcNAc–capped *O*-glycans have protective properties against *H. pylori* infection.

To test this hypothesis, we generated mucin-type glycoproteins containing terminal α1,4-GlcNAc and determined its effect on *H. pylori* in vitro. Because CD43 serves as a preferential core protein of these *O*-glycans (*8*), we generated recombinant soluble CD43 having α1,4-GlcNAc–capped *O*-glycans in transfected Chinese hamster ovary cells (*9*). Soluble CD43 without α1,4-GlcNAc was used as a control.

H. pylori (ATCC43504), incubated with the medium containing varying amounts of recombinant soluble CD43, showed little growth during the first 2.5 days, irrespective of the presence or absence of α1,4-

[1]Department of Pathology and [2]Department of Laboratory Medicine, Shinshu University School of Medicine, and [3]Institute of Organ Transplants, Reconstructive Medicine and Tissue Engineering, Shinshu University Graduate School of Medicine, Asahi 3-1-1, Matsumoto 390-8621, Japan. [4]Glycobiology Program, Cancer Research Center, The Burnham Institute, 10901 North Torrey Pines Road, La Jolla, CA 92037, USA.

*To whom correspondence should be addressed. E-mail: jun@hsp.md.shinshu-u.ac.jp

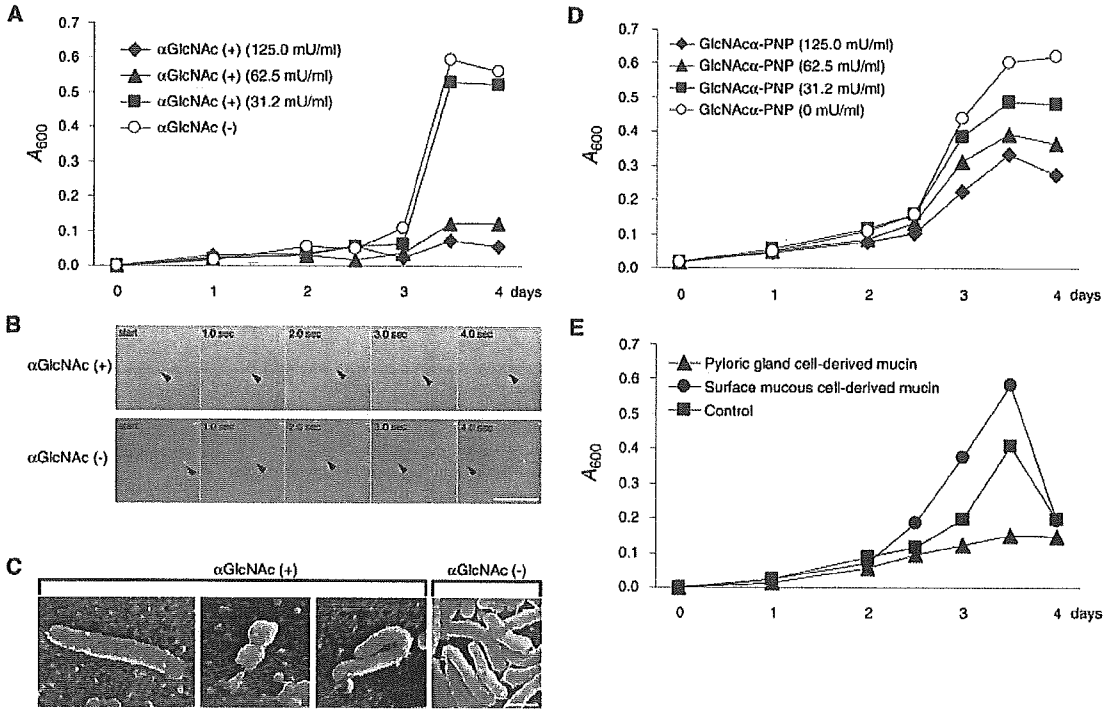

Fig. 1. α1,4-GlcNAc–capped *O*-glycans inhibit the growth and motility of *H. pylori*. (**A**) Growth curves of *H. pylori* cultured in the presence of soluble CD43 with terminal α1,4-GlcNAc [αGlcNAc (+)] or soluble CD43 without terminal α1,4-GlcNAc [αGlcNAc (–)]; the protein concentration of αGlcNAc (–) was the same as that of 125.0 mU/ml of αGlcNAc (+). One miliunit of αGlcNAc (+) corresponds to 1 μg (2.9 nmol) of GlcNAcα-PNP. A_{600}, absorbance at 600 nm. (**B**) Motility of *H. pylori* cultured with 31.2 mU/ml of αGlcNAc (+) or the same protein concentration of αGlcNAc (–) for 3 days by time-lapse recording with 1-s intervals. Representative *H. pylori* is indicated by arrowheads. The mean velocity of seven *H. pylori* cultured in the presence of αGlcNAc (+) and αGlcNAc (–) is 3.1 ± 3.5 μm/s (mean ± SD) and 21.2 ± 2.6 μm/s ($P < 0.001$). Scale bar, 50 μm. (**C**) Scanning electron micrographs of *H. pylori* incubated with 31.2 mU/ml of αGlcNAc (+) or the same protein concentration of αGlcNAc (–) for 3 days. Note abnormal morphologies such as elongation, segmental narrowing, and folding in the culture with αGlcNAc (+). All photographs were taken at the same magnification. Scale bar, 1 μm. (**D**) Growth curves of *H. pylori* cultured in the medium supplemented with various amounts of GlcNAcα-PNP. Growth of the bacteria is suppressed by GlcNAcα-PNP in a dose-dependent manner. (**E**) Growth curves of *H. pylori* cultured in the medium supplemented with pyloric gland cell-derived mucin containing 125 mU/ml of α1,4-GlcNAc or the same protein concentration of surface mucous cell-derived mucin isolated from the human gastric mucosa. The death phase started from 3.5 days, and saline instead of each mucin was supplemented as a control experiment. In (A), (D), and (E), each value represents the average of duplicate measurements.

GlcNAc–capped *O*-glycans, characteristic of the lag phase of *H. pylori* growth (Fig. 1A). After 3 days, microbes cultured in the presence of control soluble CD43 grew rapidly, corresponding to the log phase of bacterial growth. In contrast, soluble CD43 containing more than 62.5 mU/ml of terminal α1,4-GlcNAc impaired log-phase growth. Although growth inhibition was not obvious at a lower concentration (31.2 mU/ml), time-lapse images of the microbes revealed significant reduction of motility under this condition (Fig. 1B). Morphologic examination at the lower concentration revealed abnormalities of the microbe, such as elongation, segmental narrowing, and folding (Fig. 1C). These morphologic changes are distinct from conversion to coccoid form, because reduction of growth, associated with conversion from the bacillary to the coccoid form (*10*), was not apparent under these conditions. These inhibitory effects of soluble CD43 containing terminal α1,4-GlcNAc were also detected against various *H. pylori* strains, including another authentic strain, ATCC43526, and three clinical isolates with a minimum inhibitory concentration between 15.6 mU/ml and 125.0 mU/ml. By contrast, neither inhibitory growth nor abnormal morphology of *H. pylori* was observed at any concentrations of soluble CD43 lacking α1,4-GlcNAc (Fig. 1, A to C). These results indicate that α1,4-GlcNAc–capped *O*-glycans specifically suppress the growth of *H. pylori* in a manner similar to other antimicrobial agents. Similar inhibitory effects on *H. pylori* were also found in another mucin-like glycoprotein, CD34 (*11*) having terminal α1,4-GlcNAc (*12*). In addition, *p*-nitrophenyl-α-*N*-acetylglucosamine (GlcNAcα-PNP) suppressed the growth of *H. pylori* in a dose-dependent manner (Fig. 1D), although the effects were not as strong with soluble CD43 having terminal α1,4-GlcNAc (Fig. 1A). These results provide evidence that the terminal α1,4-GlcNAc residues, rather than scaffold proteins, are critical for growth inhibitory activity against *H. pylori*, and that the presentation of multiple terminal α1,4-GlcNAc residues as a cluster on mucin-type glycoprotein may be important for achieving the optimal activity.

To determine whether natural gastric mucins containing terminal α1,4-GlcNAc can also inhibit growth of *H. pylori*, subsets of human gastric mucins were prepared from the surface mucous cells and pyloric gland cells (*9*). The growth of *H. pylori* was significantly suppressed with mucin derived from pyloric gland cells at 125.0 mU/ml during the log phase (Fig. 1E). A similar inhibitory effect was also observed when the glandular mucin prepared from human gastric juice was tested (*13*). By contrast, mucin derived from surface mucous cells, MUC5AC, stimulated growth. These results support the hypothesis that natural gastric mucins containing terminal α1,4-GlcNAc, secreted from gland mucous cells, have antimicrobial activity against *H. pylori*.

The morphologic abnormalities of *H. pylori* induced by α1,4-GlcNAc–capped *O*-glycans are similar to those induced by antibiotics such as β-lactamase inhibitors, which disrupt biosynthesis of peptidoglycan in the cell wall (*14, 15*). Therefore, these *O*-glycans may inhibit cell wall biosynthesis in *H. pylori*. The cell wall of

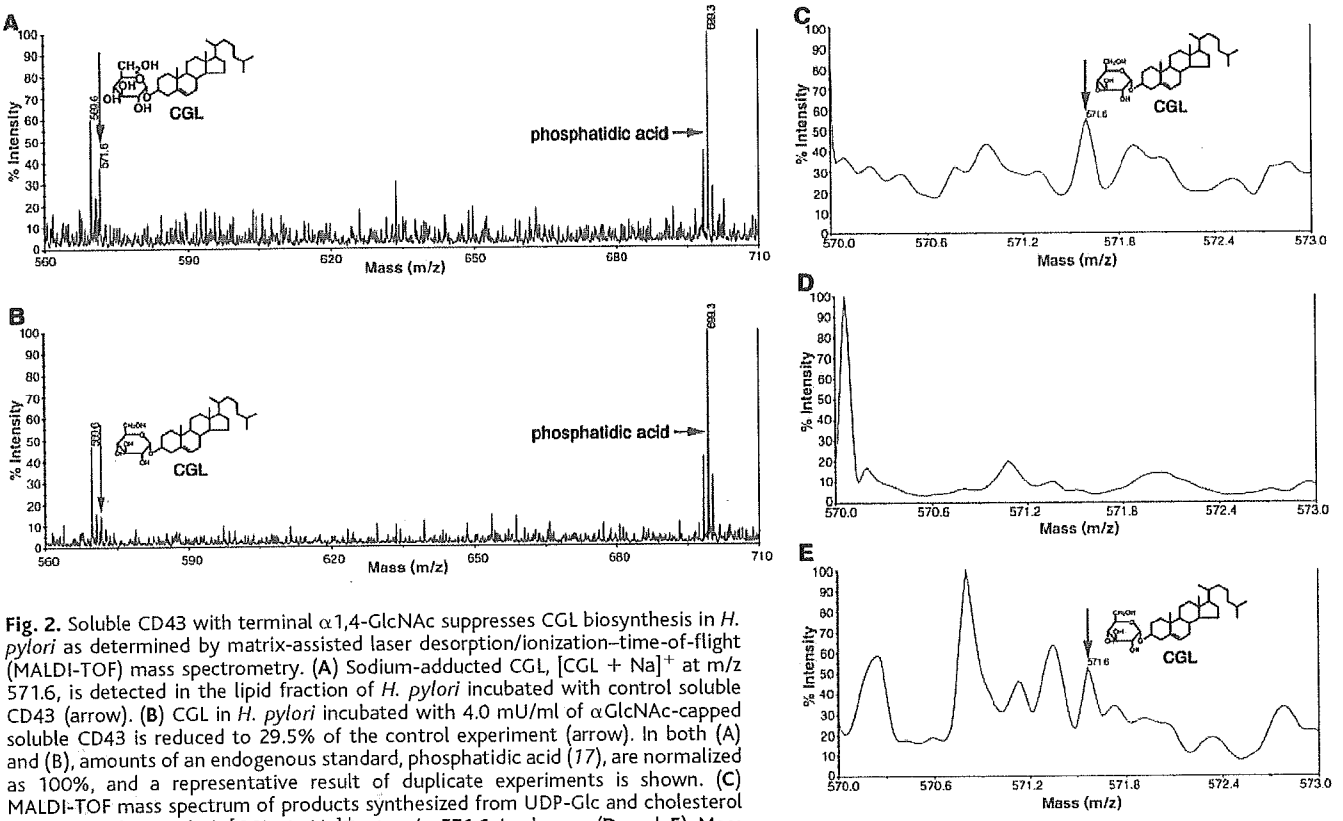

Fig. 2. Soluble CD43 with terminal α1,4-GlcNAc suppresses CGL biosynthesis in *H. pylori* as determined by matrix-assisted laser desorption/ionization–time-of-flight (MALDI-TOF) mass spectrometry. (**A**) Sodium-adducted CGL, $[CGL + Na]^+$ at m/z 571.6, is detected in the lipid fraction of *H. pylori* incubated with control soluble CD43 (arrow). (**B**) CGL in *H. pylori* incubated with 4.0 mU/ml of αGlcNAc-capped soluble CD43 is reduced to 29.5% of the control experiment (arrow). In both (A) and (B), amounts of an endogenous standard, phosphatidic acid (*17*), are normalized as 100%, and a representative result of duplicate experiments is shown. (**C**) MALDI-TOF mass spectrum of products synthesized from UDP-Glc and cholesterol by sonicated *H. pylori*. $[CGL + Na]^+$ at m/z 571.6 is shown. (**D** and **E**) Mass spectrum of products synthesized from UDP-Glc and cholesterol by sonicated *H. pylori* in the presence of 50.0 mU/ml of α1,4-GlcNAc–capped soluble CD43 (D) or control soluble CD43 (E). Note that CGL is not synthesized in the presence of α1,4-GlcNAc–capped soluble CD43 in (D).

Fig. 3. Absence of α-CGs including CAG, CGL, and CPG in *H. pylori* cultured without exogenous cholesterol. Total glycolipids extracted from *H. pylori* incubated with Brucella broth lacking cholesterol (lane 1) or containing 0.005% cholesterol (lane 2) were analyzed by thin-layer chromatography.

Helicobacter species characteristically contains α-cholesteryl glucosides (α-CGs), of which the major components are cholesteryl-α-D-glucopyranoside (CGL), cholesteryl-6-*O*-tetradecanoyl-α-D-glucopyranoside (CAG), and cholesteryl-6-*O*-phosphatidyl-α-D-glucopyranoside (CPG) (*16*). Mass spectrometric analysis of the cell wall components from *H. pylori* cultured with α1,4-GlcNAc–capped *O*-glycans displayed reduced lipid-extractable cell wall constituents (Fig. 2B). In particular, the levels of CGL, relative to phosphatidic acid (*17*), were significantly reduced as compared with controls (Fig. 2, A and B). These results suggest that α1,4-GlcNAc–capped *O*-glycans directly inhibit biosynthesis of CGL in vivo by *H. pylori*.

CGL is likely formed by a UDP-Glc:sterol α-glucosyltransferase, which transfers glucose (Glc) from UDP-Glc to the C3 position of cholesterol with α-linkage. Incubation of cholesterol and UDP-Glc with *H. pylori* lysates revealed substantial amounts of CGL by mass spectrometry (Fig. 2C), demonstrating the activity of UDP-Glc:sterol α-glucosyltransferase in *H. pylori*. When soluble CD43 containing terminal α1,4-GlcNAc was added to this assay, production of CGL was suppressed (Fig. 2D), whereas no effect was seen with control soluble CD43 (Fig. 2E). Considering structural similarity between α-linked GlcNAc found in the gland mucous cell–type mucin and the α-linked Glc found in CGL, these findings suggest that the terminal α1,4-GlcNAc residues could directly inhibit the α-glucosyltransferase activity through an end-product inhibition mechanism (*18*), resulting in decreased CGL biosynthesis.

Genes involved in the biosynthesis of cholesterol are not found in the genome database of *H. pylori* (*19*). Thus, *H. pylori* may not be able to synthesize CGL in the absence of exogenous cholesterol. When *H. pylori* was cultured for 5 days without cholesterol, bacterial growth was significantly reduced (table S1). In such cultures, *H. pylori* was elongated and no motile microbes were found. When *H. pylori* was further cultured without cholesterol for up to 21 days, the microbes died off completely. By contrast, when *H. pylori* was cultured with cholesterol, bacteria grew well, and no signs of abnormality were detected (table S1). *H. pylori* cultured with cholesterol (*9*) revealed a typical triplet of α-CGs including CGL (Fig. 3, lane 2), while α-CGs were not detected in *H. pylori* cultured without cholesterol (Fig. 3, lane 1). Moreover, no antibacterial effect of soluble CD43 containing terminal α1,4-GlcNAc was observed on bacterial strains lacking CGL such as *Escherichia coli*, *Pseudomonas aeruginosa*, *Klebsiella pneumoniae*, *Staphylococcus aureus*, α-*Streptococcus*, and *Streptococcus pneumoniae* (*9*). These results collectively indicate that synthesis of CGL by using exogenously supplied cholesterol is required for the survival of *H. pylori* and that antimicrobial activity of α1,4-GlcNAc–capped *O*-glycans may be restricted to bacterial strains expressing CGL.

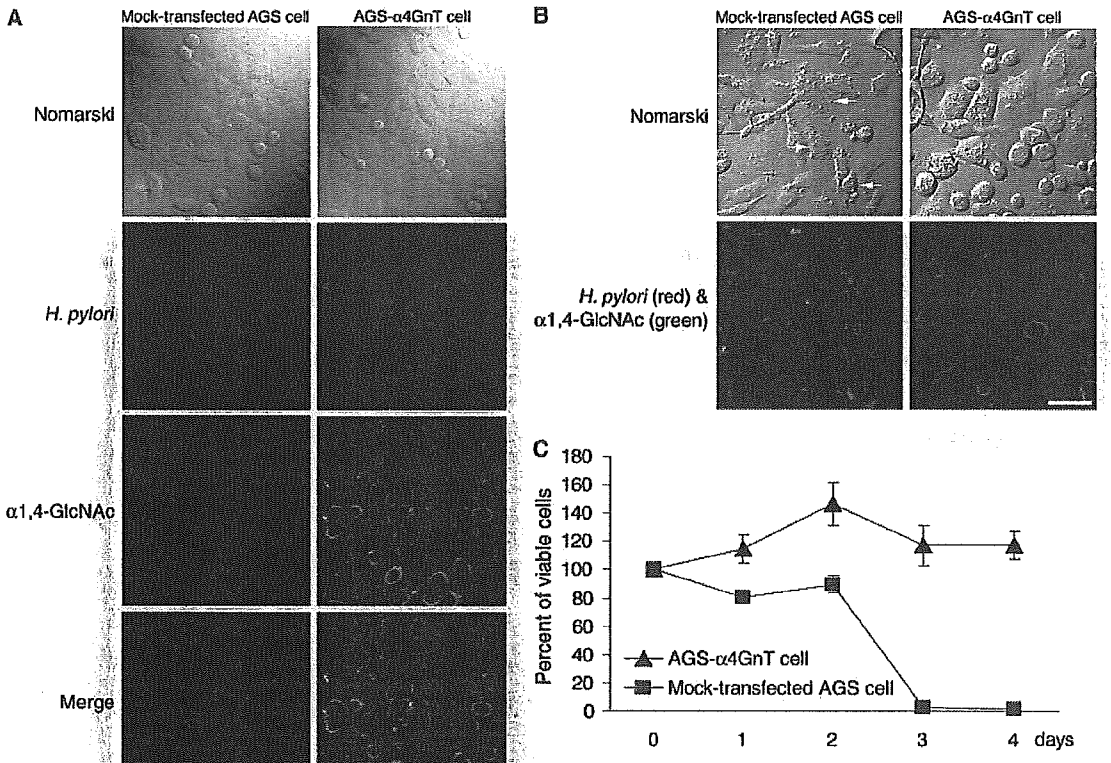

Fig. 4. α1,4-GlcNAc–capped *O*-glycans protect the host cells. AGS cells were incubated with *H. pylori* for 8 hours (**A**) or 24 hours (**B**), and doubly stained with anti-*H. pylori* antibody (red) and HIK1083 antibody specific for terminal α1,4-GlcNAc (*27*) (green). (A) Note that comparable number of *H. pylori* adhered to both mock-transfected AGS cells and AGS-α4GnT cells. (B) After 24 hours, marked damage such as cell flatness or shrinkage are noted (arrows) in mock-transfected AGS cells; no cellular damage and few attached bacteria are found in AGS-α4GnT cells. (Top) Nomarski photographs of the same field. Scale bar, 50 μm. (**C**) Viabilities of AGS cells cocultured with *H. pylori* for 4 days determined by MTS assay. Note that viability of mock-transfected AGS cells was significantly reduced after the third day, whereas AGS-α4GnT cells were fully viable for up to 4 days. The assay was done with triplicate measurements, and error bars indicate SD.

To test whether mucous cells expressing α1,4-GlcNAc–capped *O*-glycans protect themselves against *H. pylori* infection, gastric adenocarcinoma AGS-α4GnT cells stably transfected with α4GnT cDNA were cocultured with *H. pylori* (*9*). With a short-term incubation (8 hours), the microbes attached equally well to AGS-α4GnT cells and mock-transfected AGS cells. No significant damage was observed in either group of cells (Fig. 4A). Upon prolonged incubation (24 hours), mock-transfected AGS cells exhibited remarkable deterioration, such as flatness or shrinkage, with increased number of associated *H. pylori* (Fig. 4B), and the number of viable AGS cells was dramatically reduced after the third day (Fig. 4C). This cellular damage may be attributed to the perturbed signal transduction in AGS cells, where a tyrosin phosphatase, SHP-2, is constitutively activated by *H. pylori* CagA protein (*20*). By contrast, growth of *H. pylori* in cultures with AGS-α4GnT cells was markedly suppressed, and cellular damage found in mock-transfected AGS cells was barely detected in these cells (Fig. 4B). Thus, the viability of AGS-α4GnT cells was fully maintained for up to 4 days (Fig. 4C). These results indicate that α1,4-GlcNAc–capped *O*-glycans have no effect on the adhesion of *H. pylori* to AGS-α4GnT cells, but protect the host cells from *H. pylori* infection.

Glycan chains play diverse roles as ligands for cell surface receptors (*11*, *21*–*23*) and as modulators of receptors and adhesive proteins (*24*–*26*). The present study reveals a new aspect of mammalian glycan function as a natural antibiotic. Because α1,4-GlcNAc–capped *O*-glycans are produced by human gastric gland mucous cells, the present study provides a basis for development of novel and potentially safe therapeutic agents to prevent and treat *H. pylori* infection in humans without adverse reactions.

References and Notes

1. R. M. Peek Jr., M. J. Blaser, *Nature Rev. Cancer* **2**, 28 (2002).
2. D. R. Cave, *Semin. Gastrointest. Dis.* **12**, 196 (2001).
3. P. Sipponen, H. Hyvarinen, *Scand. J. Gastroenterol. Suppl.* **196**, 3 (1993).
4. H. Ota *et al.*, *Histochem. J.* **23**, 22 (1991).
5. E. Hidaka *et al.*, *Gut* **49**, 474 (2001).
6. D. Ilver *et al.*, *Science* **279**, 373 (1998).
7. J. Mahdavi *et al.*, *Science* **297**, 573 (2002).
8. J. Nakayama *et al.*, *Proc. Natl. Acad. Sci. U.S.A.* **96**, 8991 (1999).
9. Materials and methods are available as supplemental material on *Science* Online.
10. H. Enroth *et al.*, *Helicobacter* **4**, 7 (1999).
11. J.-C. Yeh *et al.*, *Cell* **105**, 957 (2001).
12. M. Kawakubo, J. Nakayama, unpublished observations.
13. Y. Ito, M. Kawakubo, J. Nakayama, unpublished observations.
14. T. Horii *et al.*, *Helicobacter* **7**, 39 (2002).
15. J. Finlay, L. Miller, J. A. Poupard, *J. Antimicrob. Chemother.* **52**, 18 (2003).
16. Y. Hirai *et al.*, *J. Bacteriol.* **177**, 5327 (1995).
17. Y. Inamoto *et al.*, *J. Clin. Gastroenterol.* **17**, S136 (1993).
18. J. Nakayama *et al.*, *J. Biol. Chem.* **271**, 3684 (1996).
19. J. F. Tomb *et al.*, *Nature* **388**, 539 (1997).
20. H. Higashi *et al.*, *Science* **295**, 683 (2002).
21. J. B. Lowe, *Cell* **104**, 809 (2001).
22. T. O. Akama *et al.*, *Science* **295**, 124 (2002).
23. N. L. Perillo, K. E. Pace, J. J. Seilhamer, L. G. Baum, *Nature* **378**, 736 (1995).
24. D. J. Moloney *et al.*, *Nature* **406**, 369 (2000).
25. M. Demetriou, M. Granovsky, S. Quaggin, J. W. Dennis, *Nature* **409**, 733 (2001).
26. J. Nakayama, M. N. Fukuda, B. Fredette, B. Ranscht, M. Fukuda, *Proc. Natl. Acad. Sci. U.S.A.* **92**, 7031 (1995).
27. K. Ishihara *et al.*, *Biochem. J.* **318**, 409 (1996).

28. This work was supported by a Grant-in-Aid for Scientific Research on Priority Area 14082201 from the Ministry of Education, Culture, Sports, Science and Technology of Japan (J.N.) and by grants CA 71932 (M.N.F.) and CA 33000 (M.F.) from the National Cancer Institute. The authors thank H. Ota, Y. Kawakami, T. Taketomi, and O. Harada for discussions; E. Ruoslahti, R. C. Liddington, and E. Lamar for critical reading of the manuscript; and E. Hidaka, Y. Takahashi, S. Kubota, and A. Ishida for technical assistance. This report is dedicated to the memory of Hideki Matsumoto.

Supporting Online Material

www.sciencemag.org/cgi/content/full/305/5686/1003/DC1

Materials and Methods

Table S1

References and Notes

16 April 2004; accepted 21 June 2004

Clinical utility of quantitative RT-PCR targeted to α1,4-*N*-acetylglucosaminyltransferase mRNA for detection of pancreatic cancer

Satoshi Ishizone,[1] Kazuyoshi Yamauchi,[2] Shigeyuki Kawa,[3] Takefumi Suzuki,[2] Fumiaki Shimizu,[1] Oi Harada,[4] Atsushi Sugiyama,[1] Shinichi Miyagawa,[1] Minoru Fukuda[6] and Jun Nakayama[4,5,7]

Departments of [1]Surgery, [2]Laboratory Medicine, [3]Internal Medicine and [4]Pathology, Shinshu University School of Medicine; [5]Institute of Organ Transplants, Reconstructive Medicine and Tissue Engineering, Shinshu University Graduate School of Medicine, Asahi 3-1-1, Matsumoto 390-8621, Japan; and [6]Glycobiology Program, Cancer Research Center, Burnham Institute for Medical Research, 10901 North Torrey Pines Road, La Jolla, CA 92037, USA

(Received August 29, 2005/Revised October 30, 2005/Accepted November 3, 2005/Online publication January 23, 2006)

α1,4-*N*-Acetylglucosaminyltransferase (α4GnT) is a glycosyltransferase responsible for the biosynthesis of α1,4-GlcNAc-capped *O*-glycans, and is frequently expressed in pancreatic cancer cells but not peripheral blood cells. In the present study, we tested the clinical utility of α4GnT mRNA expressed in the mononuclear cell fraction of peripheral blood as a biomarker of pancreatic cancer. Total RNA isolated from the peripheral blood mononuclear cells from 55 pancreatic cancer patients, 10 chronic pancreatitis patients, and 70 cancer-free volunteers was analyzed quantitatively by reverse transcription-polymerase chain reaction with primers specific for α4GnT, and the expression level of α4GnT mRNA relative to that of glyceraldehyde-3-phosphate dehydrogenase (GAPDH) was measured. When the ratio of α4GnT to GAPDH transcripts exceeded a defined cut-off value, patients were considered to have pancreatic cancer. By these standards, 76.4% of the pancreatic cancer patients were detected by this assay. A strong correlation was obtained between positivity in this assay and the expression of α4GnT protein detected immunohistochemically in pancreatic cancer tissues resected subsequently, suggesting that α4GnT mRNA detected in the peripheral blood is derived from circulating pancreatic cancer cells. Although increased levels of α4GnT mRNA was detected in 40.0% of chronic pancreatitis patients and 17.1% of cancer-free volunteers, the expression levels were significantly lower than those seen in pancreatic cancer patients. These results suggest that quantitative analysis of α4GnT mRNA expressed in the mononuclear cell fraction of peripheral blood will contribute to the detection of pancreatic cancer. (*Cancer Sci* 2006; 97: 119–126)

Pancreatic cancer is one of the most intractable malignancies.[1,2] In particular, the 5-year survival rate of this neoplasm is the lowest of all types of cancer, and it is the fifth leading cause of cancer death in Japan.[3] The poor prognosis of pancreatic cancer is largely attributable to the difficulty in diagnosis of the disease at relatively early stages as well as the highly invasive character of the cancer cells, regardless of the tumor size. In fact, the vast majority of pancreatic cancer patients are diagnosed at advanced stages associated with clinical manifestations such as jaundice and back pain, likely due to the limitation of tumor markers available for the diagnosis of pancreatic cancer at potentially curable stages.[4] Several well-established biomarkers, including CEA,[5] CA19-9,[6] DU-PAN-2[7,8] and Span-1,[9] are available for the detection of pancreatic cancer, but it is also true that these biomarkers are not elevated in certain numbers of pancreatic cancer patients. Thus, in order to detect pancreatic cancer more efficiently, it is necessary to identify novel biomarkers that will be useful for its diagnosis.[10,11]

Mucous glycoproteins secreted from the gastroduodenal mucosa are heavily glycosylated and protect the mucosa against various pathogens and physical stresses. Among the oligosaccharides found in human gastrointestinal mucins, α1,4-GlcNAc-capped *O*-glycan is unique because its expression in normal tissues is limited to gastric gland mucous cells, Brunner's gland of the duodenal mucosa and accessory gland of the pancreaticobiliary tract.[12] Interestingly, this unique *O*-glycan is expressed frequently in neoplastic cells such as carcinomas of the stomach, bile duct and pancreas, as well as pancreatic intraepithelial neoplasia (PanIN-I, PanIN-II and PanIN-III),[13] thus it is regarded as a tumor-associated carbohydrate antigen for these tumors.[12] Recently we isolated a cDNA encoding human α4GnT, which is responsible for the biosynthesis of α1,4-GlcNAc-capped *O*-glycans, by expression cloning from a gastric mucosa cDNA library.[14] We subsequently demonstrated that α4GnT is expressed in the Golgi of gastric gland mucous cells and Brunner's glands in normal gastroduodenal mucosa as well as the Golgi of adenocarcinoma cells such as gastric, pancreatic and biliary tract cancers expressing α1,4-GlcNAc-capped *O*-glycans.[15–17]

Our previous study demonstrated that neither α4GnT RNA nor protein is detectable in the normal peripheral blood cells.[17] Thus, we quantitatively measured the expression levels of α4GnT mRNA in the mononuclear cell fraction of peripheral blood obtained from gastric cancer patients using RT-PCR and demonstrated that this assay is useful to detect, as well as monitor, gastric cancer.[17] The present study extends this assay for detection of pancreatic cancer using a technically

[7]To whom correspondence should be addressed. E-mail: jun@hsp.md.shinshu-u.ac.jp
Abbreviations: α4GnT, α1,4-*N*-Acetylglucosaminyltransferase; GAPDH, glyceraldehyde-3-phosphate dehydrogenase; H. pylori, Helicobacter pylori; MTC, multiple tissue cDNA; ROC, receiver operating characteristic; RT-PCR, reverse transcription–polymerase chain reaction; TAMURA, 3′-6-carboxy-*N*,*N*,*N*′,*N*′-tetramethylrhodamine; TBS, Tris buffered saline.

doi: 10.1111/j.1349-7006.2006.00148.x

improved modification. Specifically, levels of α4GnT mRNA in the mononuclear cell fraction of peripheral blood from pancreatic cancer patients were determined quantitatively using multiplex PCR employed to detect simultaneously both α4GnT and an internal standard gene in a single reaction tube.

Materials and Methods

Clinical samples

The present study involved 55 pancreatic cancer patients (34 men and 21 women; age range 45–92 years [mean ± SE, 68.5 ± 9.8 years]). For the reduction of jaundice, a drainage tube was placed in the common bile duct of 16 of 32 patients whose tumors were located in the pancreatic head, whereas none of the 23 patients whose tumor was located in the body or tail of the pancreas received such drainage. In addition to the pancreatic cancer patients, samples from 10 chronic pancreatitis patients (10 men; ages ranging from 55 to 75 years [65.8 ± 7.6]) and 70 volunteers (70 men; ages ranging from 31 to 90 years [69.4 ± 1.4]) were analyzed. These volunteers underwent a health screening and were verified to be cancer-free by routine examinations including abdominal ultrasonography. Written informed consent was obtained from all patients and volunteers prior to the study. Peripheral blood samples were taken from patients and volunteers. In pancreatic cancer patients, blood samples were collected before surgical resection of the primary tumor. When patients underwent endoscopic biopsy of the gastric mucosa, blood samples were taken minimally at 2-week intervals after biopsy.

In addition to the patients' samples, the Human Blood Fractions MTC Panel of the first-strand cDNA (Clontech, Palo Alto, CA, USA) was analyzed. This panel is composed of mononuclear cells (B cells, T cells and monocytes) pooled from 50 male or female Caucasians, resting $CD8^+$ cells pooled from 33 male or female Caucasians, resting $CD4^+$ cells pooled from 20 male or female Caucasians, resting $CD14^+$ cells pooled from 36 male or female Caucasians, resting $CD19^+$ cells pooled from 34 male or female Caucasians, $CD19^+$ cells activated with pokeweed mitogen pooled from four male or female Caucasians, mononuclear cells activated with pokeweed mitogen and concanavalin A pooled from four male or female Caucasians, $CD4^+$ cells activated with concanavalin A pooled from 12 male or female Caucasians, and $CD8^+$ cells activated with phytohemagglutinin pooled from eight male or female Caucasians. These samples were analyzed using a real-time quantitative RT-PCR assay. In parallel, tissue specimens of pancreatic cancer obtained from 23 patients who subsequently underwent surgical operation for removal of primary tumors were examined by immunohistochemistry, and the tumor stage was classified according to the tumor node metastasis classification system.[18] In addition, pancreatic tissue specimens of two cases operated for chronic pancreatitis were archived from the pathology files of Shinshu University Hospital, Matsumoto, Japan. The study protocol was approved by the Institutional Review Board of Shinshu University School of Medicine.

RNA extraction and cDNA synthesis

Five milliliters of peripheral blood was collected, treated with ethylene diamine tetraacetic acid to prevent coagulation, and layered on 3 mL of Lymphprep (Nycomed Pharma, Oslo, Norway) in a 15-mL polypropylene tube. The tube was centrifuged at 2000*g* for 30 min at 20°C. The mononuclear cell fraction was transferred to a new tube, resuspended in 5 mL phosphate-buffered saline, and then centrifuged at 3000*g* for 5 min. Total RNA was isolated from the pellet using a RNeasy Mini kit (Qiagen, Valencia, CA, USA), followed by DNaseI treatment. After inactivation of DNaseI, 11 μL of the DNaseI-treated RNA was incubated with 1 μL of 10 mM dNTPs and 1 μL of 0.5 mg/mL oligo$(dT)_{15}$ primer (Promega, Madison, WI, USA) at 65°C for 5 min. After chilling on ice, these mixed samples were then incubated with 4 μL of 5× first strand buffer, 1 μL of 0.1 M dithiothreitol, 1 μL of RNase inhibitor (Promega), and 1 μL of the reverse transcriptase SuperScript 2 (Invitrogen, Carlsbad, CA, USA) at 42°C for 1 h. The reaction was terminated by heating at 70°C for 15 min, and samples were then kept at −20°C until real-time quantitative RT-PCR analysis.

Real-time RT-PCR

Quantitation of α4GnT mRNA expressed in peripheral blood mononuclear cells as well as the Human Blood Fractions MTC Panel was carried out using an ABI PRISM 7700 Sequence Detection System (PE Applied Biosystems, Foster City, CA, USA) as described previously, with minor modifications.[17] On the basis of the published human *α4GnT* sequence,[14] specific primer pairs and probes were designed using the Primer Express program (PE Applied Biosystems). Forward and reverse primers for human *α4GnT* were 5′-GTTTTCCTCTTCCC-TTTGGATATGA-3′ (nucleotides +340 to +364; the first nucleotide of the initiation methionine codon is +1) and 5′-AGCTGATGTGGAGCCAGTTTCT-3′ (nucleotides +427 to +448), respectively. These primers were designed to hybridize to different exons of the *α4GnT* gene to avoid amplifying genomic DNA. The TaqMan probe was synthesized as 5′-TGGTACAATCAAATCAACGCCAGCGC-3′ (nucleotides +397 to +422) by PE Applied Biosystems, and it carried a 5′-6-carboxyfluorescein reporter label and a TAMURA quencher group. To normalize α4GnT mRNA expression levels, a housekeeping gene, *GAPDH*, was quantitatively analyzed simultaneously as a control. To construct a standard curve, 10-fold dilutions of the plasmid cDNA harboring *α4GnT* (pcDNAI-α4GnT) ranging from 3×10^{-2} to 3×10^{-10} μg/mL, corresponding to 5×10^9 to 5×10^1 copies/mL were prepared. Similarly, a 10-fold dilution of the plasmid cDNA harboring a partial cDNA sequence of *GAPDH* (pCR2.1-GAPDH), which was constructed as described previously,[17] was prepared from 2.3×10^{-2} to 2.3×10^{-10} μg/mL, corresponding to 5×10^9 to 5×10^1 copies/mL.

Multiplex PCR was carried out in 50 μL of reaction mixture containing 3 μL of cDNA sample, 25 μL of 1× Universal PCR Master Mix (PE Applied Biosystems), 800 nM of the primer set for α4GnT, 80 nM of the primer for *GAPDH*, 125 nM of the TaqMan probe for *α4GnT*, and 100 nM of the TaqMan probe for *GAPDH* that carries the 5′-VIC reporter label and 3′-TAMURA quencher group (PE Applied Biosystems). Reaction tubes were placed in the ABI PRISM 7700 Sequence Analyzer, preheated at 95°C for 10 min and amplified for 50 cycles of 95°C for 15 s, followed by 60°C for 1 min. The abundance of α4GnT mRNA and GAPDH mRNA was determined by comparison with the standard curves for

doi: 10.1111/j.1349-7006.2006.00148.x

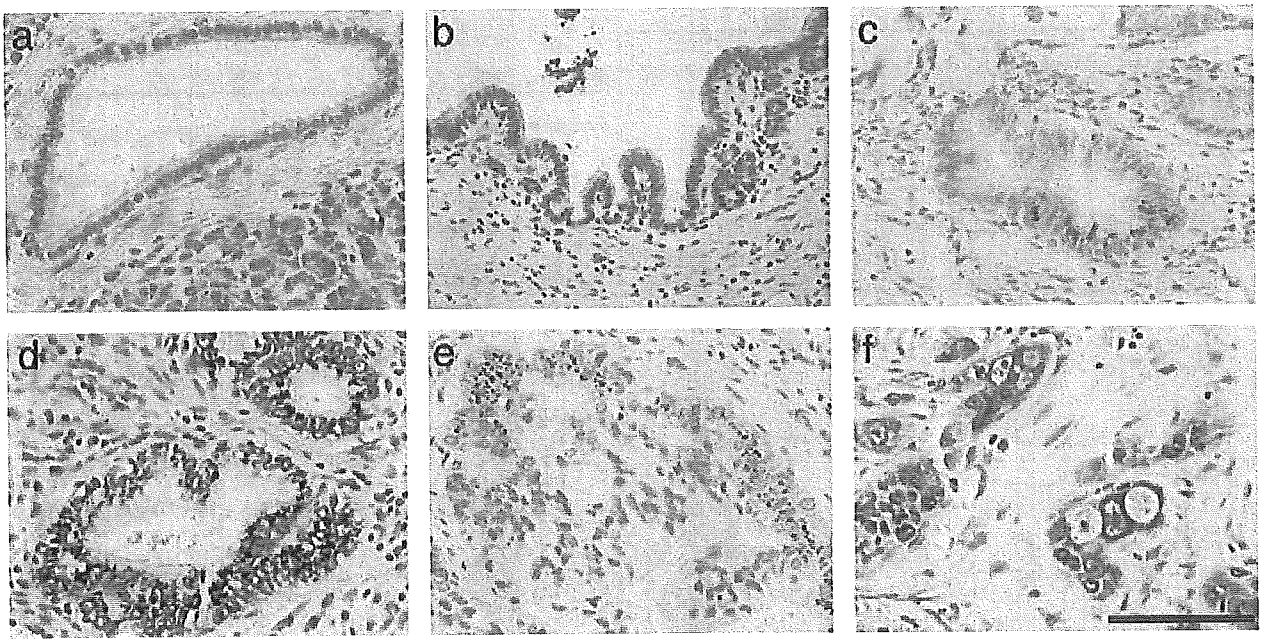

Fig. 1. Expression of α4GnT protein in the normal and neoplastic pancreatic tissues. α4GnT was detected by immunohistochemistry using the antiα4GnT antibody I17K. α4GnT is not expressed in the normal pancreatic duct (a), whereas it is expressed in the Golgi region of pancreatic ducts exhibiting PanIN-IB (b). The α4GnT protein is also expressed in the pancreatic ducts with PanIN-II found in chronic pancreatitis (c). In the pancreatic carcinoma, α4GnT protein is detected in well differentiated (d), moderately differentiated (e), and poorly differentiated (f) adenocarcinomas. Scale bar = 100 μM.

α4GnT and GAPDH, respectively, and the relative expression level of α4GnT mRNA was defined by multiplying the α4GnT : GAPDH mRNA ratio by 1.0×10^7. The assays were carried out in duplicate, and mean values of the two experiments were indicated.

Immunohistochemistry

To detect α4GnT protein in pancreatic cancer cells, 23 cases of the resected pancreatic cancer tissues were subjected to immunohistochemistry with the monospecific antiα4GnT polyclonal antibody, I17K, as described previously.[16] Briefly, 3 μM-thick sections were deparaffinized and treated with 0.3% H_2O_2 in methanol and then blocked with 1% normal goat serum in TBS. The sections were incubated with the antibody for 1.5 h. After washing with TBS, sections were incubated with biotinylated antirabbit IgG and then horseradish peroxidase-labeled streptavidin. The peroxidase reaction was developed with a diaminobenzidine/H_2O_2 solution, and counterstained with hematoxylin. In control experiments carried out by replacing the primary antibody with preimmune serum or omitting the primary antibody from the staining procedure, no specific staining was seen. Tissue specimens containing > 5% positively stained cancer cells were defined as positive, and the others were classified as negative according to previously described criteria.[19]

Enzyme immunoassay of biomarkers in patients' serum

Various biomarkers, including CEA, CA19-9, DU-PAN-2 and Span-1, in pancreatic cancer patients' serum were evaluated by enzyme immunoassay before surgery. CEA (cut-off value, 2.5 ng/mL) was measured using a CEA•Dainapack kit (Dainabot, Tokyo, Japan), and CA19-9 (cut-off value, 37 U/mL) was measured using an AxSYM CA19-9•Dainapack kit (Dainabot). DU-PAN-2 (cutoff value, 150 U/mL) and Span-1 (cutoff value, 30 U/mL) were measured by SRL at Tokyo, Japan.

Statistics

Statistical analyses comparing two independent groups categorized by the clinicopathological variables of pancreatic cancer were carried out using the Mann–Whitney *U*-test. Similarly, comparisons among more than three groups were carried out using the Kruskal–Wallis test. These analyses were performed using StatView 5.0 software (Abacus Concepts, Berkeley, CA, USA). In addition, a cut-off value was determined by constructing a ROC curve using StatMate III (ATMS, Tokyo, Japan). Statistical association between the expression of α4GnT protein in the resected pancreatic cancer tissues and the expression level of α4GnT mRNA determined in the mononuclear cell fraction of peripheral blood was evaluated using Fisher's test (Abacus Concepts). In these analyses, *P*-values < 0.05 were considered to be statistically significant.

Results

Expression of α4GnT protein in pancreatic cancer cells

In order to determine the expression of α4GnT protein in pancreatic ductal adenocarcinoma cells, immunohistochemistry using the antiα4GnT antibody I17K was undertaken with normal and neoplastic tissues of the pancreas, which were resected surgically at the time of operation. In the normal pancreas, α4GnT was not detected in the main or interlobular pancreatic ducts (Fig. 1a). By contrast, α4GnT protein was

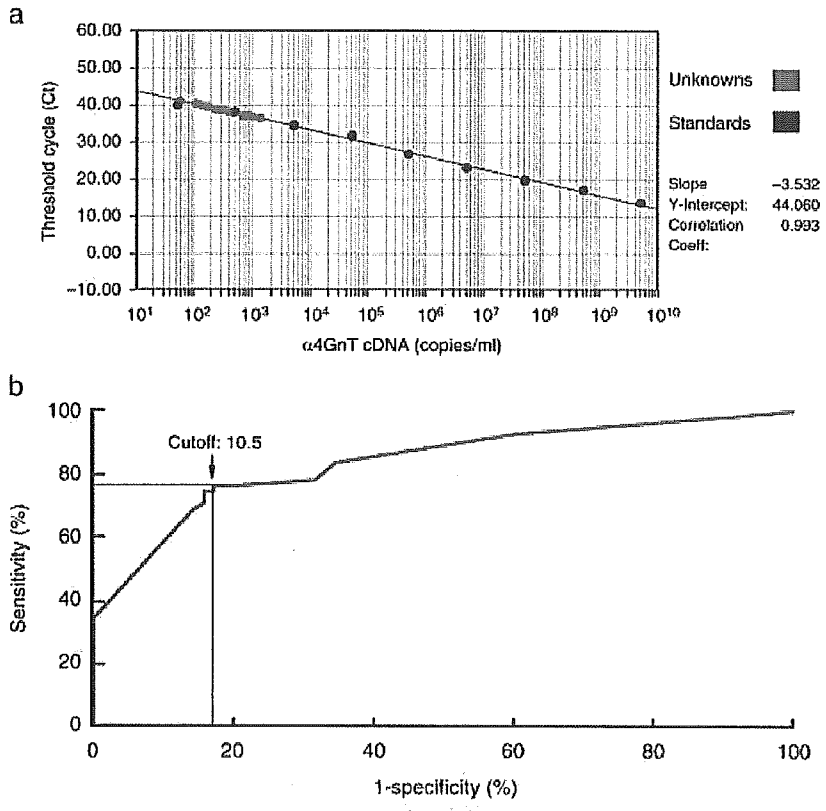

Fig. 2. Quantitative RT-PCR assay targeting α4GnT mRNA. (a) A standard curve for α4GnT was constructed by plotting serially diluted α4GnT cDNA, pcDNAI-α4GnT (black dots), where unknown samples from patients or cancer-free volunteers are indicated as red dots. (b) ROC curve was created by plotting the expression level of α4GnT mRNA in the peripheral blood from 55 pancreatic cancer patients and 70 cancer-free volunteers. Arrow denotes the cutoff value of 10.5, which best discriminates pancreatic cancer patients from cancer-free volunteers with 76.4% sensitivity and 82.9% specificity.

associated with the Golgi region of pancreatic ducts with PanIN-IB (Fig. 1b). α4GnT protein was also expressed in the pancreatic ducts with PanIN-II found in the inflammatory lesions of chronic pancreatitis in both of the two cases examined (Fig. 1c). In pancreatic cancer, α4GnT was detected in the Golgi of adenocarcinoma cells in 73.9% of 23 patients, irrespective of histological tumor type; that is, five of nine patients with well-differentiated adenocarcinoma (Fig. 1d), seven of eight patients with moderately differentiated adenocarcinoma (Fig. 1e) and five of six patients with poorly differentiated adenocarcinoma (Fig. 1f) were positive for α4GnT protein in cancer tissues.

Construction of a standard curve for the quantitative RT-PCR assay

The standard curve for α4GnT mRNA was constructed using 10-fold dilutions of α4GnT cDNA, pcDNAI-α4GnT (Fig. 2a). By defining the cycle number where fluorescence reached a detection threshold as Ct, we obtained a strong linear relationship between Ct and the log of the cDNA concentration. Based on the standard curve, levels of α4GnT mDNA ranging from 5×10^1 to 5×10^9 copies/mL were detected in a reaction tube. Similarly, GAPDH mRNA was detected ranging from 5×10^1 to 5×10^9 copies/mL based on the standard curve for GAPDH constructed using 10-fold dilutions of pCR2.1-GAPDH. Using these standard curves, the expression level of α4GnT mRNA relative to that of GAPDH mRNA was determined.

Determination of a cut-off value distinguishing pancreatic cancer patients from cancer-free volunteers

To most efficiently discriminate pancreatic cancer patients from cancer-free volunteers, a ROC curve was constructed (Fig. 2b). Thus, the α4GnT:GAPDH mRNA ratios multiplied by 1.0×10^7 were defined as the expression level of α4GnT, and the values determined in the mononuclear cell fraction of the peripheral blood from 55 patients with pancreatic cancer versus 70 cancer-free volunteers were plotted. By defining the cut-off value as 10.5, the optimal combination of 76.4% for sensitivity and 82.9% for specificity was obtained. Thus, we regarded a value as positive when expression levels of α4GnT mRNA greater than 10.5 were obtained in this assay.

Determination of the expression levels of α4GnT mRNA in peripheral blood samples from pancreatic cancer patients and cancer-free volunteers

Based on the criterion that the expression level of α4GnT mRNA should exceed the cut-off value of 10.5 for a positive result in this assay, we determined the expression levels of α4GnT mRNA in the mononuclear cell fraction of peripheral blood isolated from 55 pancreatic cancer patients and 70 cancer-free volunteers (Fig. 3).

In pancreatic cancer, 42 (76.4%) of 55 patients examined were positive for this assay, and the expression level of α4GnT mRNA was 37.50 ± 5.44 (mean ± SE). The expression level of α4GnT transcripts was then evaluated by clinicopathological variables including tumor location, stage, venous invasion,

doi: 10.1111/j.1349-7006.2006.00148.x

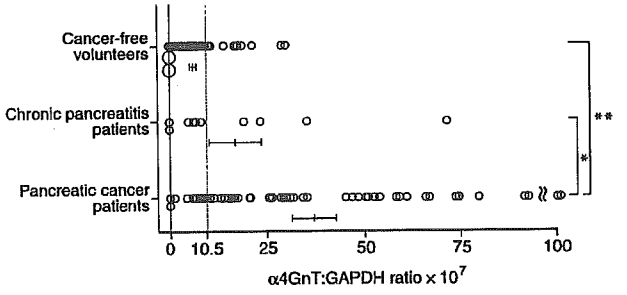

Fig. 3. Scatter plots indicating the expression level of α4GnT mRNA in the mononuclear cell fraction of peripheral blood measured by the quantitative RT-PCR. Small and large circles represent one and 10 individuals, respectively. Horizontal bars indicate mean ± SE. *$P < 0.05$, **$P < 0.001$.

lymphatic invasion and lymph node metastasis determined at subsequent surgical operation. Although the frequency of the positive patients and the expression level of α4GnT seemed to be associated with tumor progression, no significant statistical differences were seen in any clinicopathological variables examined (Table 1).

In addition, the expression level of α4GnT mRNA in the mononuclear cell fraction of blood samples from cancer-free volunteers was determined. Of the 70 cancer-free volunteers examined, 12 (17.1%) volunteers were found to be positive for this assay, but the expression level of α4GnT transcripts was 7.2 ± 0.9, which was significantly lower than that seen in pancreatic cancer patients ($P < 0.001$).

We then tested whether activated lymphocytes express α4GnT mRNA aberrantly by using the Human Blood Fractions MTC Panel, and it was shown that α4GnT mRNA was not detectable in any of the blood fractions examined, including activated lymphocytes.

Detection of α4GnT mRNA in peripheral blood samples from chronic pancreatitis patients

We next measured the expression level of α4GnT in the mononuclear cell fraction of peripheral blood isolated from chronic pancreatitis patients (Fig. 3). Of the 10 patients examined, four (40.0%) were classed as positive by exceeding the defined cutoff of 10.5. However the expression level of α4GnT mRNA was found to be 17.87 ± 6.98, which was again significantly lower than that seen in pancreatic cancer patients ($P < 0.05$). Statistically significant differences between expression levels were not seen between cancer-free volunteers and chronic pancreatitis patients.

Comparison of α4GnT mRNA with well-characterized biomarkers in pancreatic cancer patients

The results of the real-time PCR analysis of α4GnT mRNA expressed in the mononuclear cell fraction of peripheral blood from the pancreatic cancer patients were then compared with the results of enzyme immunoassays for well-characterized biomarkers including CEA, CA19-9, DU-PAN-2 and Span-1. As shown in Table 2, more than 74% of pancreatic patients were positive for either α4GnT or CA19-9, and CEA and DU-PAN-1 were found to less frequently detect pancreatic cancer compared with α4GnT and CA19-9.

Table 1. Frequency of pancreatic cancer patients positive for the α4GnT assay and correlation between expression levels of α4GnT mRNA in peripheral blood mononuclear cells and clinicopathological variables

Variable	Frequency of positive patients[†]		α4GnT mRNA[‡] (mean ± SE)	*P*-value
	n	%		
Tumor location				
Head	25/32	78.1	37.95 ± 7.03	0.9728[§]
Body and tail	17/23	73.9	36.87 ± 8.78	
Tumor stage				
0	0/1	0	5.290	0.4571[¶]
II	2/3	66.7	29.44 ± 11.67	
III	7/8	87.5	32.85 ± 8.55	
IV	33/43	76.7	39.68 ± 6.72	
Venous invasion				
Negative	3/5	60.0	29.29 ± 11.20	0.6954[§]
Positive	17/19	89.5	36.97 ± 10.36	
Lymphatic invasion				
Negative	1/3	33.3	11.81 ± 4.82	0.0606[§]
Positive	19/21	90.5	38.74 ± 9.44	
Lymph node metastasis				
Negative	5/7	71.4	28.78 ± 9.93	0.8241[§]
Positive	15/17	88.2	38.09 ± 11.32	

[†]Expression levels greater than 10.5 were defined as positive.
[‡]α4GnT:GAPDH mRNA ratios multiplied by 1.0×10^7 are indicated.
[§]Analyzed using the Mann–Whitney *U*-test. [¶]Analyzed using the Kruskal–Wallis test.

We then tested whether a combined assay with α4GnT and another biomarker would detect pancreatic cancer patients more efficiently than the enzyme immunoassays targeting single biomarkers (Table 3). Notably, it was found that more than 86% of pancreatic cancer patients were detected when the α4GnT assay was combined with enzyme immunoassay for CEA, CA19-9, DU-PAN-2 or Span-1. In particular, 96.4% of pancreatic cancer patients were positive for either α4GnT mRNA or Span-1 or both, whereas 71.4% of the patients were positive for Span-1 alone.

Detection of α4GnT protein in resected pancreatic cancer tissues

Transcripts of α4GnT are not detectable in peripheral blood cells, including leukocytes, lymphocytes and monocytes.[17] Thus, it is possible that α4GnT mRNA detected in the mononuclear cell fraction of peripheral blood from pancreatic cancer patients is derived from circulating pancreatic cancer cells expressing α4GnT mRNA. To test this hypothesis, the results of real-time RT-PCR of α4GnT mRNA expressed in the peripheral blood were compared with those of α4GnT protein expressed in 23 cases of the subsequently resected pancreatic cancer tissues by immunohistochemistry with the antiα4GnT antibody I17K. In 19 patients positive for α4GnT transcripts in the peripheral blood, 17 were also positive for α4GnT protein in the resected pancreatic cancer tissues. By contrast, α4GnT protein was not detected in pancreatic cancer tissues of three of four patients who were also negative for the α4GnT mRNA assay. These results indicate a significant association between α4GnT mRNA in the peripheral blood

Table 2. Frequency of pancreatic cancer patients detected using assays for α4GnT mRNA, CEA, CA19-9, DU-PAN-2 and SPan-1

Tumor stage	α4GnT mRNA (> 10.5)		CEA (> 2.5 ng/mL)		CA19-9 (> 37 U/mL)		DU-PAN-2 (> 150 U/mL)		SPan-1 (> 30 U/mL)	
	n	%	*n*	%	*n*	%	*n*	%	*n*	%
0	0/1	0	0/1	0	0/1	0	NE	NE	NE	NE
II	2/3	66.7	0/3	0	0/3	0	0/2	0	0/2	0
III	7/8	87.5	3/8	37.5	6/8	75.0	1/8	12.5	2/7	28.6
IV	33/43	76.7	23/41	56.1	34/42	82.9	16/22	72.7	18/19	94.7
Total	42/55	76.4	26/53	49.1	40/54	74.1	17/32	53.1	20/28	71.4

NE, not evaluated.

Table 3. Frequency of pancreatic cancer patients detected using combined assays†

Biomarker	CEA (> 2.5 ng/mL)		CA19-9 (> 37 U/mL)		DU-PAN-2 (> 150 U/mL)		SPan-1 (> 30 U/mL)	
	n	%	*n*	%	*n*	%	*n*	%
α4GnT mRNA	46/53	86.8	48/54	88.9	30/32	93.8	27/28	96.4
CEA	–	–	43/53	81.1	24/32	75.0	21/28	75.0
CA19-9	–	–	–	–	27/32	84.4	23/28	82.1
DU-PAN-2	–	–	–	–	–	–	21/28	75.0

†Frequency of the patients positive for either or both biomarkers combined is indicated.

and α4GnT protein in pancreatic cancer tissues ($P = 0.0209$), suggesting that α4GnT mRNA detected in patients' peripheral blood is derived from circulating pancreatic cancer cells.

Discussion

α1,4-*N*-Acetylglucosaminyltransferase is a glycosyltransferase that mediates the transfer of GlcNAc with an α1,4-linkage from UDP-GlcNAc to βGal residues, forming α1,4-GlcNAc-capped *O*-glycans.[14] As shown in our previous studies and confirmed here, α4GnT is expressed frequently in pancreatic cancer cells as well as in gastric cancer cells, but not in peripheral blood cells.[15,17] Therefore, we used quantitative RT-PCR to determine the expression level of α4GnT mRNA in tumor cells circulating in the peripheral blood of pancreatic cancer patients. We primarily defined the cut-off value as 10.5 for this assay, based on the ROC curve, and could detect 76.4% of 55 pancreatic cancer patients. The significant correlation between the expression level of α4GnT mRNA in the peripheral blood detected by the RT-PCR assay and α4GnT protein detected in resected pancreatic cancer tissues by immunohistochemistry strongly suggests that α4GnT mRNA detected in the peripheral blood is derived from circulating pancreatic cancer cells. Although 40% of 10 chronic pancreatitis patients and 17.1% of 70 cancer-free volunteers were also positive by this assay, the expression levels of α4GnT mRNA in both groups were significantly lower than those seen in pancreatic cancer patients. These results indicate the clinical utility of real-time RT-PCR targeted to α4GnT mRNA for detection of pancreatic cancer.

The present study also revealed that the location of the pancreatic tumor does not alter the results of the assay (Table 1). It is known that early detection of pancreatic cancer occurring in the tail and body of the pancreas can be particularly difficult because jaundice, which is frequently associated with pancreatic head cancer, is not evident unless the common bile duct is affected by the tumor.[1] Thus, the assay demonstrated here will likely contribute to early detection of pancreatic body and tail cancers that are not associated with jaundice.

In the present study, we have also shown that the expression level of α4GnT mRNA in the peripheral blood from pancreatic cancer patients is elevated in a manner correlated with tumor stage (Table 1), suggesting that the number of cancer cells entering the peripheral blood is increased as the tumor progresses. Most recently, we have shown that α1,4-GlcNAc-capped *O*-glycans secreted from gastric gland mucous cells function as an antibiotic against *H. pylori* infection.[20] The role of these unique *O*-glycans expressed on pancreatic cancer cells remains unknown, and thus further study will be required to address this problem.

There are several biomarkers for pancreatic cancer, including CEA,[5] CA19-9,[6] DU-PAN-2[7,8] and Span-1.[9] Among them, CA19-9 is the most widely used in screening and monitoring of the disease.[21–24] We compared α4GnT with other biomarkers (including CA19-9) and found that the frequency of pancreatic cancer patients detected by α4GnT was much the same as that detected by CA19-9 (Table 2). The same analysis also revealed that DU-PAN-2 and CEA detected pancreatic cancer patients less frequently than α4GnT, CA19-9 and Span-1. It is noteworthy that two of three patients at stage II were positive for α4GnT mRNA, suggesting the possible usefulness of α4GnT mRNA for the early detection of pancreatic cancer. Further study on a larger number of patients with stages 0, I and II will be required to prove this possibility.

The present study demonstrated that the frequency of pancreatic cancer patients detected using enzyme immunoassays for CEA, CA19-9, DU-PAN-2 and Span-1 was increased substantially when combined with the α4GnT assay (Table 3). It is generally accepted that the quantitative RT-PCR assay requires much time and cost compared with enzyme immunoassay.

doi: 10.1111/j.1349-7006.2006.00148.x